For Reference

NOT TO BE TAKEN FROM THIS ROOM

Ex libris
universitatis
albertaensis

For Reference

NOT TO BE TAKEN FROM THIS ROOM

The University of Alberta
Printing Department
Edmonton, Alberta


Digitized by the Internet Archive
in 2020 with funding from
University of Alberta Libraries

https://archive.org/details/DAJohnston1968

THE UNIVERSITY OF ALBERTA

A PHASE-LOCKED TRANSPONDER SYSTEM FOR TELEMETERING THE POSITION OF WILD ANIMALS

by

(C) DONALD A. JOHNSTON

A THESIS

SUBMITTED TO THE FACULTY OF GRADUATE STUDIES

IN PARTIAL FULFILMENT OF THE REQUIREMENTS FOR THE DEGREE

OF MASTER OF SCIENCE

DEPARTMENT OF ELECTRICAL ENGINEERING

EDMONTON, ALBERTA

SEPTEMBER, 1968

THE UNIVERSITY OF ALBERTA

A PHASE-LOCKED TRANSPONDER SYSTEM FOR TELEMETERING
THE POSITION OF WILD ANIMALS

by

(C) DONALD A. JOHNSTON

A THESIS

SUBMITTED TO THE FACULTY OF GRADUATE STUDIES
IN PARTIAL FULFILLMENT OF THE REQUIREMENTS FOR THE DEGREE
OF MASTER OF SCIENCE

DEPARTMENT OF ELECTRICAL ENGINEERING

EDMONTON, ALBERTA
SEPTEMBER, 1968

THESIS
1968 (F)
108

UNIVERSITY OF ALBERTA

FACULTY OF GRADUATE STUDIES

The undersigned certify that they have read and recommend to the faculty for acceptance, a thesis entitled A Phase-Locked Transponder System for Telemetering the Position of Wild Animals, submitted by Donald A. Johnston in partial fulfilment of the requirements for the degree of Master of Science.

ACKNOWLEDGEMENTS

The research described in this thesis was carried out at the Department of Electrical Engineering, University of Alberta under the supervision of E. M. Edwards and Dr. C. G. Englefield.

The author wishes to thank Mr. Edwards, who concieved of and guided this project, and Dr. Englefield, whose suggestions have changed the course of the work at critical times, and the staff and graduate students of the Department for their assistance.

The author is further indebted to the University and the National Research Council for financial assistance.

ACKNOWLEDGEMENTS

The research described in this thesis was carried out at the Department of Electrical Engineering, University of Alberta under the supervision of E. M. Edwards and Dr. G. G. Engelfield.

The author wishes to thank Mr. Edwards, who conceived of and guided this project, and Dr. Engelfield, whose suggestions have changed the course of the work at critical times, and the staff and graduate students of the Department for their assistance.

The author is further indebted to the University and the National Research Council for financial assistance.

ABSTRACT

A system is proposed for tracking coyotes in the wild by radio telemetry. Instead of the conventional simple transmitter on the animal and several observer's receivers, a transponder and its base station are to be used. The location of the animal is given by its distance and direction from the one observer's station.

A description of the distance measuring part of the system, which was built and tested in the laboratory, is given. This part of the system is found to measure the length of a cable accurately. The transponder uses a time-shared phase locked technique, measuring distance by measuring the phase shift between a 10 KHz signal generated at the observer's station and this signal received and returned by the transponder.

The required radio frequency components are to be added in later work, including receivers, transmitters and a direction finding antenna.

TABLE OF CONTENTS

LIST OF FIGURES

LIST OF TABLES

CHAPTER 1

INTRODUCTION

1.1 Telemetering the Position of an Animal

The Department of Wildlife Ecology, University of Wisconsin, operates a wildlife research station at Rochester, Alberta. A study of cyclical variations in the population of snowshoe hares is being conducted there. In order to assess the influence of coyotes and lynx on the hare population, it is desired to use radio telemetry of the movements of these predators. The Department of Electrical Engineering, University of Alberta has undertaken the development of a suitable system, and this thesis is a report of the results to date. A working telemetry system has been built in the laboratory, under which conditions it will measure the length of a cable. To this system must be added the radio frequency components.

It has become standard practice to put a collar bearing a transmitter on the animal's neck. The position of this transmitter is then determined by triangulating on it with two or more receivers, using the null in the receiving pattern of a loop antenna to locate the animal's angular position from each one. This information is used by an

observer who plots it on a map.

This system has the advantage of simplicity of the instrument on the animal. However, the transmitter must operate at all hours of the day, whether or not anyone is using the information, which means that most transmitter energy is wasted. Triangulation is a very inconvenient procedure, although a computer program has been written to make a plot of large amounts of data. (Ref.1) The accuracy of the loop is limited to about 1/2 degree (Ref.2) and with only 2 receivers the accuracy is bad either between the receivers or at a large distance from both receivers. To correct this a system with 36 antennas has been used.

As an alternative, it was suggested that the instrument on the animal be a transponder. A transponder has a receiver which awaits a signal from an observer's station. It then responds by activating its transmitter and returning a short burst of transmission bearing the information requested by the observer's station. In this case this is the travel time of the signal, which gives the distance between the two stations. An angular measurement can then be made, as with the simple transmitter, and the animal's position is then known.

Since the transponder doesn't transmit unless it is interrogated and the receiver can be made to operate on very little standby power, this system can be made to have

much longer battery life and/or less weight than the usual continuously operating transmitter. Only one observer's station will be needed and the information will be obtained directly in polar coordinates, a more readily usable form. It has the disadvantage of increased collar complexity.

1.2 Transponders

1.2.1 Pulse Transponder

The pulse type transponder has a receiver which is usually on, awaiting a signal. When a signal is received, this activates the transponder's transmitter. A short burst of energy (a reply pulse) is radiated and the receiver is activated again and begins listening for another pulse. The received pulses normally come from the observer's station and occur in trains. The observer's station has, as well as the transmitter that sends the interrogating pulses to the transponder, a receiver which listens for the transponder's reply. Additional circuitry in this station measures the time interval between the sent and received pulses at the observer's station. When the response times of the various parts of the system are subtracted the remaining time measured gives the distance, as in radar.

1.2.2 Phase Shift Transponder

This type of transponder measures distance by observing the time lag or phase shift between two signals at the base station, as shown in Fig. 1.1.

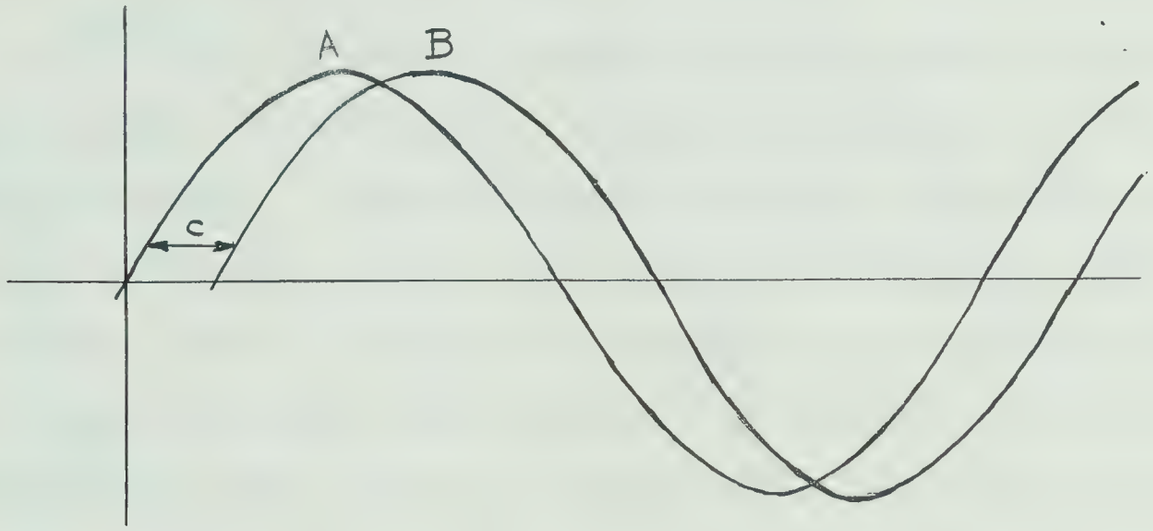

A: Base Station Signal

B: Transponder Response

C: Phase Shift due to Travel Time

Fig 1.1 Measurement of Distance by Phase Shift

The observer's station transmits a carrier modulated by a periodic signal, shown as a sine wave here, to the transponder's receiver. The transponder's transmitter returns a reply, a signal of the same frequency as the observer's station interrogation signal. The phase relation between these signals is known. At the observer's station this reply is picked up by a receiver. Additional circuitry measures the phase difference between it and the original

signal and subtracts the system phase shifts. The resulting phase shift is displayed to the observer as distance.

1.3 Frequency Selection

The problem of transmission of signals in the bush environment in which this system will operate will require further study. The efficiencies of small loops will be low and will increase as the fourth power of frequency according to Chute (Ref. 3) although Cochrane and Lord (Ref.4) use a 3.5 power law when the antenna is on the neck of an animal. Preliminary measurements by Green (Ref. 5) and data given by Terman (Ref. 6) indicate severe attenuation increasing sharply with frequency. A sketch of the expected received power is shown in Fig. 1.2.

The frequency of the minimum in power losses is not known until bush losses have been measured, but it is expected to be between 3 and 300 MHz. As is indicated by Fig. 1.2, this frequency will tend to be higher for smaller loops or smaller distances. At Cedar Creek (Ref. 2) 150 MHz was used, giving a maximum range of 3 miles on a fox.

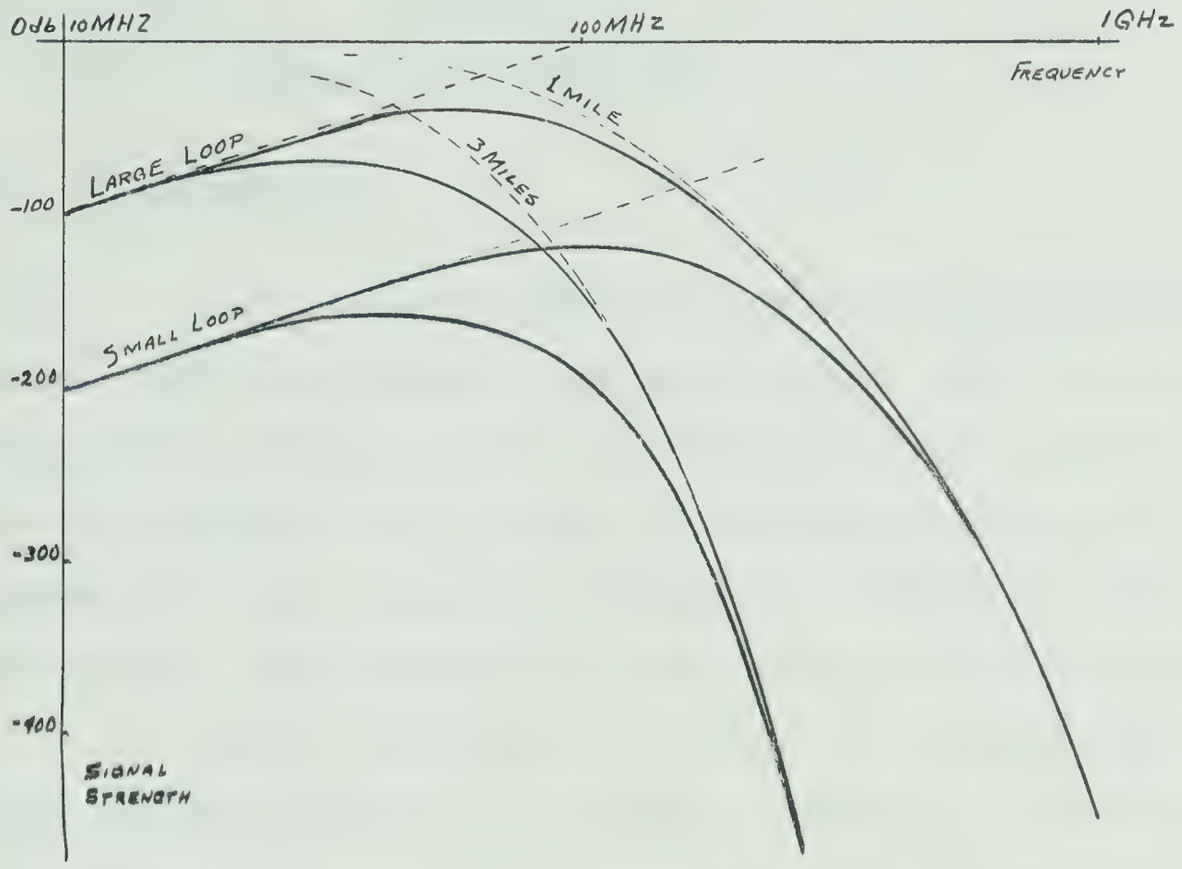

Fig. 1.2 Expected Losses

1.4 Desired Accuracy

It is desired to be able to interrogate an animal, under field conditions, at 4 to 5 miles and plot its location to within 1/8 mile. Since this system will be used at Rochester, Alberta, it should retain this accuracy over a temperature range of -50 to +50 degrees centigrade (Ref.7).

CHAPTER 2

CHOICE OF SYSTEM TYPE

2.1 Introduction

It is desirable that the efficiency of the antenna be as high as possible to gain range, and to prevent degradation of the signals the noise included should be as low as possible. To exclude noise the bandwidth of the system, or the range of frequencies included, must be minimized. The frequency will be chosen as in Sec. 1.3.

To deal with these variables it is convenient to introduce the concept of Q of the antenna. Q is given by the operating frequency divided by the antenna bandwidth (if the antenna is properly tuned). High Q gives good noise rejection and efficiency, but is found to limit distance resolution in the case of the pulse type transponder, while ideally this is not the case for the phase shift transponder.

2.2 Antennas

Chute (Ref. 3) has discussed several types of antennas to select a torque antenna and has concluded that factors arising from the manner in which it is proposed to use the antenna will dictate the final choice of antenna type. In this problem, the lowest loss loading coil for a

whip antenna mounted on the animal will be a large one, ie. a loop around the neck of the animal. The whip cannot be too long or it will interfere with the animal. It should have a good ground plane below it or it will not work properly. A loop antenna around his neck will likely have a loss of the same order of magnitude as the coil for the whip and it will be degraded only 3 db if the ground plane is absent. It will be less bothersome to the animal. In its shielded balanced form the resonant frequency can be expected to stay more stable. Thus it was decided to design the system on the assumption that a loop antenna would be used. Another type that should be considered is the ferrite rod antenna.

2.3 Loop Efficiency

The radiation resistance is given by Chute (Ref. 3) as:

$$r = 3.075 \times 10^{5} \ (a/\lambda)^{4}$$

where a is the loop diameter and λ is the wavelength. The size of the loop is determined by the animal's neck and will be about 10 cm in the case of a coyote. The wavelength is about 10 m at 30 MHz, and $r = 3 \times 10^{-3}$ Ohms. The ideal Q, Q_i is defined as that Q which would be measured if the only losses in the antenna were the radiation losses. This is $\omega L/r$ or 550,000 L where L is the inductance of the antenna in

microhenrys, typically between 0.1 and 1 microhenry for the antennas built in the lab. The efficiency is given by

$$eff = r/(r+R)$$

Q is defined by $\omega L/(r+R)$, where R is the resistance of the loop plus the series equivalent resistance of all other losses, and L is the inductance of the loop. (See Fig. 2.1.) Therefore

$$eff = Q/Q_l$$

This shows that degrading Q degrades power output as indicated in the introduction and reduces useful range.

2.4 Response Time of the Antenna

If a signal is suddenly applied to a sharply tuned antenna, potential energy must be stored in its inductance and capacitance. This means that the amplitude of the signal, or the envelope of its peaks, grows exponentially rather than instantaneously (Fig. 2.1). In the pulse type transponder the receiver must have a threshold below which signals, noise in particular, will not interrogate the transponder and waste battery life. If the received pulse is strong, the envelope is large and the receiver is triggered soon after the pulse arrives. If the signal is weak the circuit does not respond until the antenna signal has risen well up on the envelope, and a time uncertainty occurs.

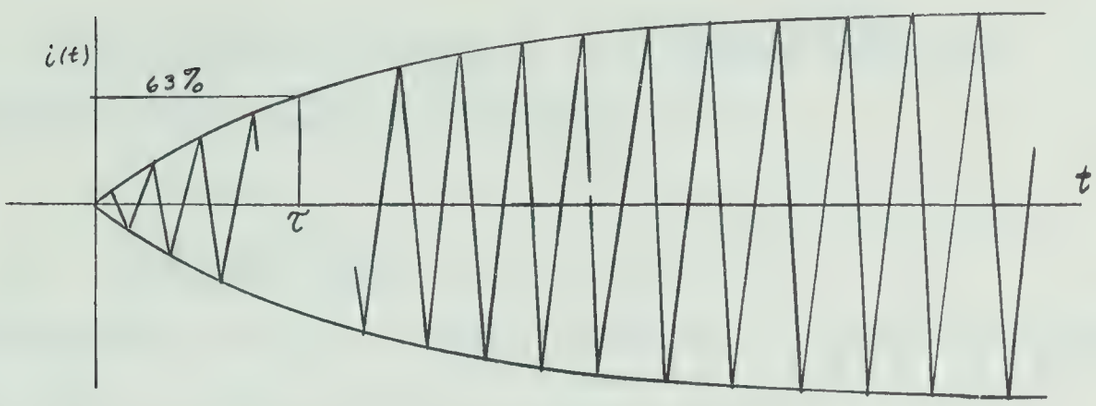

Fig. 2.1 Antenna Response

Assume that the threshold of the receiver is 63% of the final value of the envelope. This is a weak signal, within 4 db of not interrogating the transponder. Its time delay is conveniently equal to the time constant of the envelope, which will now be derived. To analyse the antenna we model it as in the circuit of Fig. 2.2.

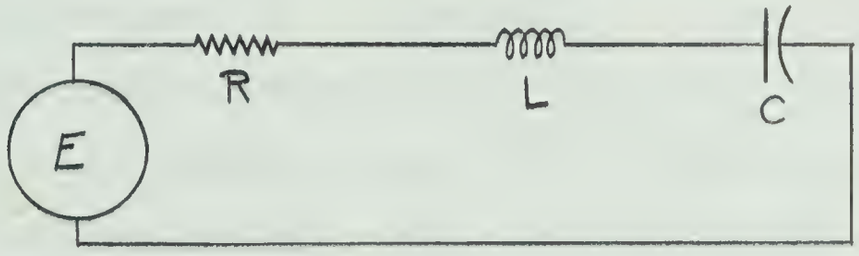

Fig. 2.2 Model of the Antenna

The current in the loop, which will be proportional to the antenna output, is given by:

$$I(s)/E(s) = pR_o/(p^2 + p/Q + 1)$$

where $E(s) = E_o s/(s^2+\omega_o^2)$, a cosine burst,

$$\omega_o = \sqrt{1/LC} \qquad Q = \omega_o L/R$$

$$p = \omega/\omega_o \qquad R_o = \sqrt{L/C}$$

The time domain response is given by

$$i(t) = E_o \omega_o R_o (\cos \omega_o t - e^{-t\omega_o/2Q} \cos \sqrt{1 - 1/4Q^2}\, \omega_o t)$$

and the time constant for large Q is:

$$\tau = 2Q/\omega_o$$

$$= 0.318\ Q/f_o$$

This implies that Q must be small for short rise time, in opposition to the efficiency requirement.

2.5 Choice of Transponder Type

In order to resolve 1/8 mile we require 660 nsec. rise time, assuming all the error to be due to the transponder antenna. This implies that Q = 56 for a 27 MHz carrier, and the efficiency is 0.1% for a 0.1 microhenry loop, which was found to be typical, and the rise time should be reduced by a factor of 2 to allow for the observer's station antenna and stray phase shifts. Going to 300 MHz would permit antenna Q's of 560, which is a more reasonable restriction, but bush losses were expected to nullify this gain. The bandwidth for 330 nsec. rise time is over 6 MHz. For a phase shift transponder, allowing for an infinite time for the sinusoidal signals to be established, the phase information can be carried by a single audio frequency and the noise bandwidth is zero. For a practical system, assuming that 6 KHz is actually used, as was later found to be reasonable, 30 db of signal to noise ratio will be gained, giving about 35 db of overall improvement in the

sensitivity of the system. Thus it was decided to design a phase shift transponder system.

2.6 Frequency of Transponder Signal

The phase shift of a periodic wave is meaningful to the observer's station only to one cycle, beyond which it becomes ambiguous whether the animal is in the distance covered by that cycle or some subsequent cycle. This means that the system should cover the full range in the first cycle. This requirement conflicts with the accuracy requirement since percentage error of phase shift measurement, at audio frequencies, doesn't depend on frequency, while distance covered is inversely proportional to frequency. Thus extending the unambiguous range by lowering the frequency reduces the accuracy in feet. Since radio waves travel approximately 1 foot per nsec. a 10 KHz frequency gives an unambiguous range of about 9 1/2 miles. It can be heard for direction measurements. For large animals it will be possible to add a second tone to extend the range. For example, a 1 KHz tone will reach 100 miles and the 10 KHz tone, phase locked to it, can still resolve the same distance, acting, so to speak, to magnify any of the ten 10-mile intervals.

2.7 Separation of Signals

In a collar the receiver antenna will be in the near field of the transmitter antenna if indeed they are not the same antenna. Modulation on the transmitter that gets into the receiver will be detected. If this modulation in turn is impressed on the transmitter, the system can oscillate. Two methods of separating the two signals were considered. It was first attempted to transmit and receive on two different frequencies with filters doing the separation. Experiments showed that this would be very difficult on a collar with power levels about 120 db different. It was decided to use time separation of the two signals (ie. time-sharing of the information channel).

2.8 The Phase Locked Method

In this technique the receiver and transmitter in either station do not operate simultaneously. The receiver in the transponder first stores received phase information in an audio oscillator by phase-locking (synchronizing) it to the incoming signal. After locking is completed the oscillator then returns this information via the transmitter while the base station receives. A circuit in the base station measures the phase difference between the returned wave and the original wave and displays it on a meter after

corrections for phase shifts in the system.

The final choice is a system using a time-shared phase-locked transponder. It operates on a 10 KHz frequency, measuring distance by the phase shift technique. A test system was built and is described in the balance of this thesis.

CHAPTER 3

THE LABORATORY SYSTEM

3.1 General

To demonstrate the transponder system decided upon, a transponder and a base station were built in two separate laboratory racks. Rather than sending the signals from one to the other by radio transmission, which would require better receivers than were available, the two units were made to communicate with each other via a cable. The signals used were the audio tone bursts (as shown in Figs. 3.3 and 3.4), transmitted by the cable without being modulated onto a radio frequency carrier. To test the operation of the system the length of the cable was measured.

Block diagrams of the two units are shown in Fig. 3.1 and Fig. 3.2. Typical waveforms are shown in Figs. 3.3 and 3.4. In this system the base station transmitted a 32 cycle burst of 10 KHz sine wave and the transponder returned 16 cycles of the locked signal. The measuring circuits of the base station rejected the first cycle of this burst and used the next 7 cycles for phase measurement. For clarity only one quarter of each tone burst is shown in Figs. 3.3 and 3.4. For details of the OA1, OA3, and OA4 see Sec. 4.1.

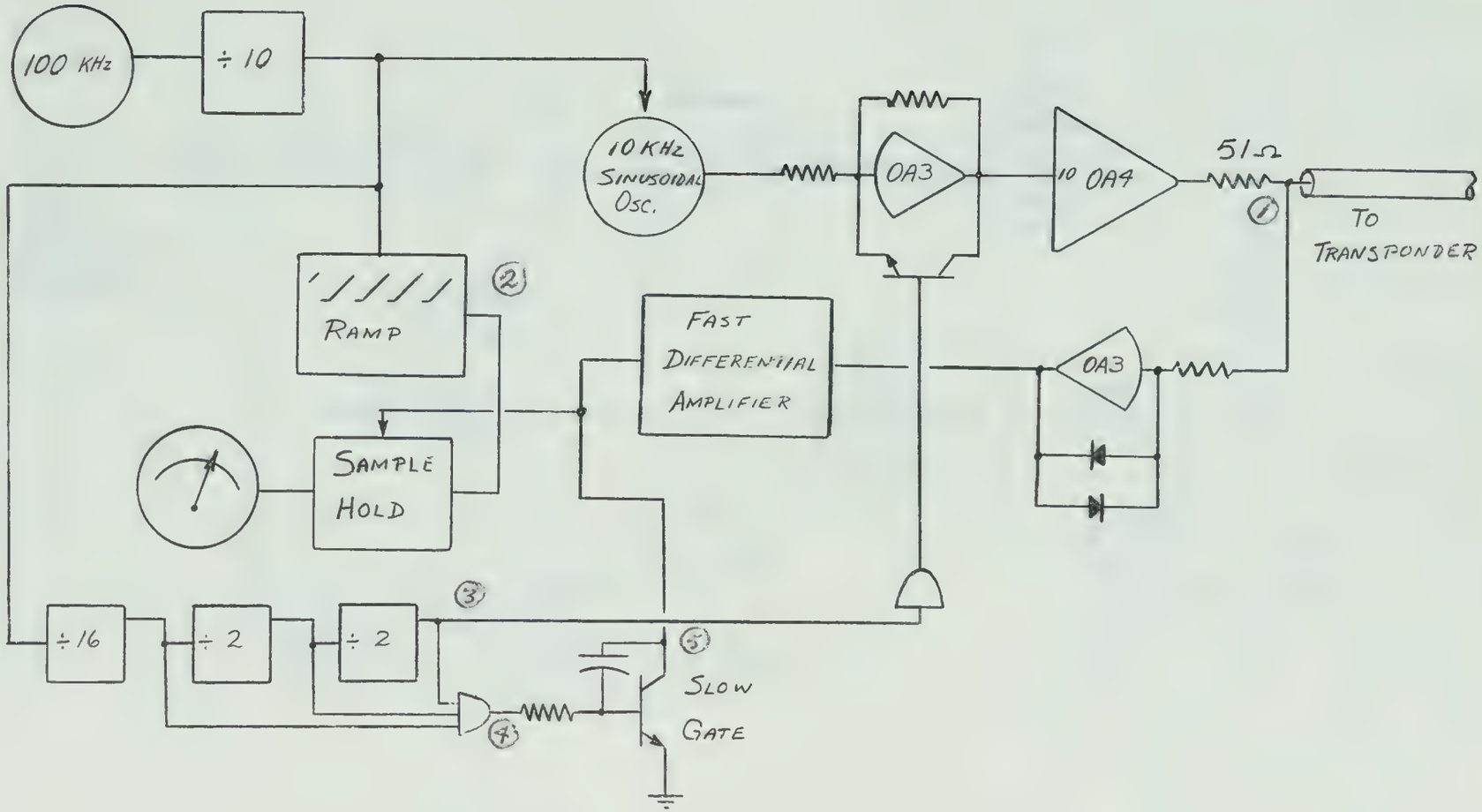

Fig. 3.1 Base Station in Test System

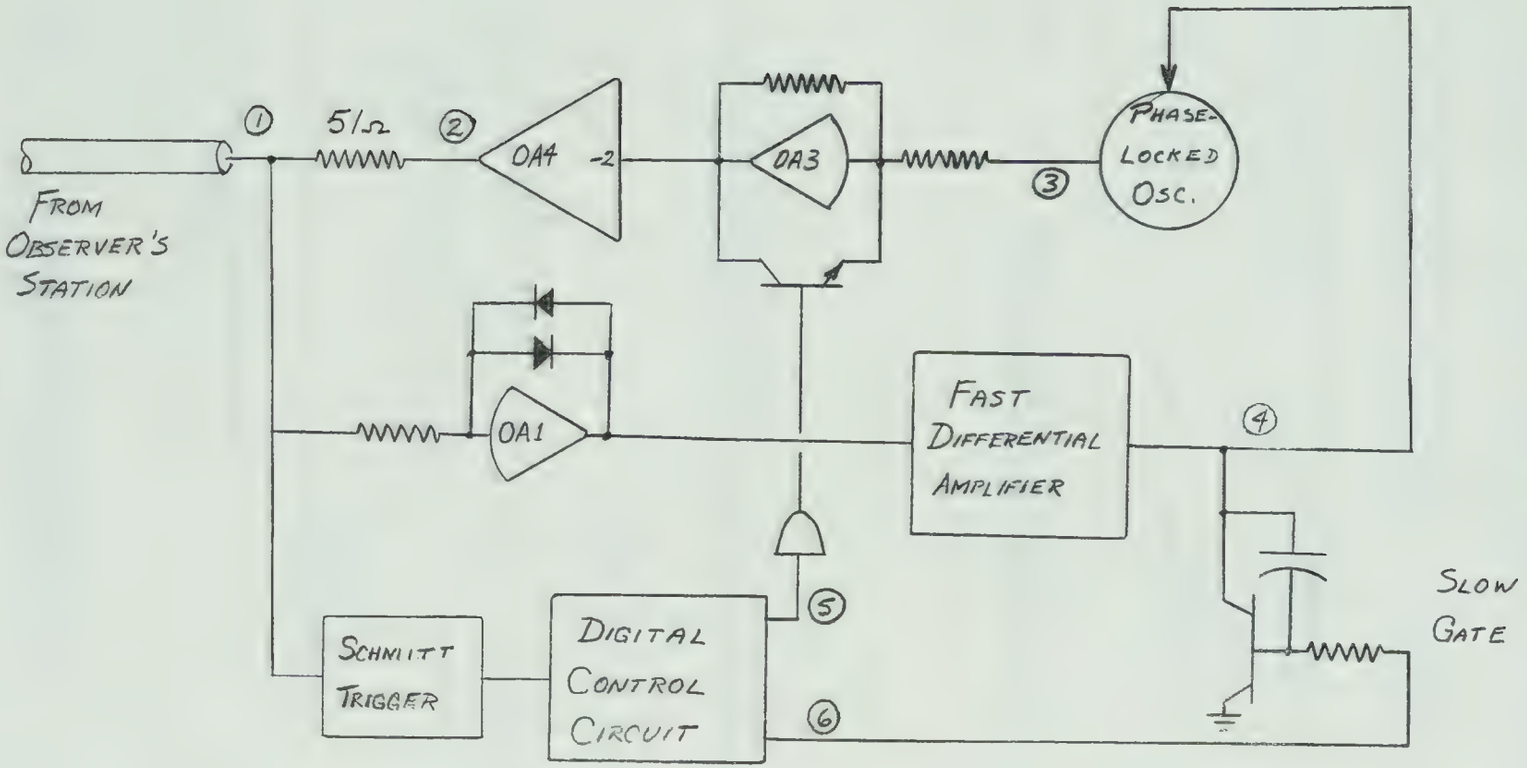

Fig. 3.2 Transponder in Test System

Typical Waveforms at Numbered Points

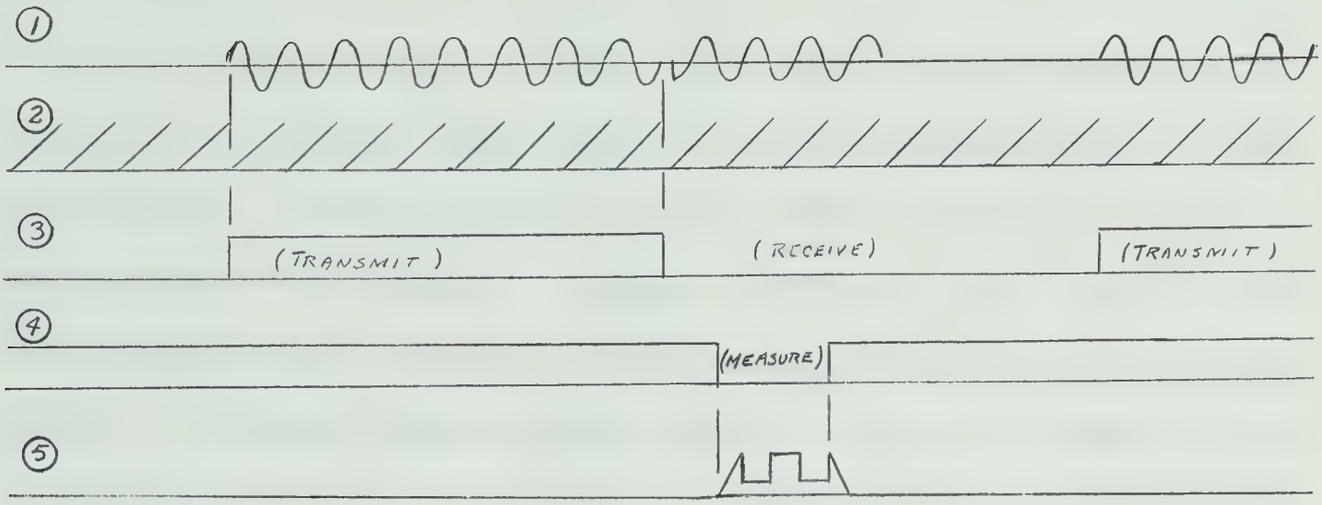

Fig. 3.3 Base Station Waveforms

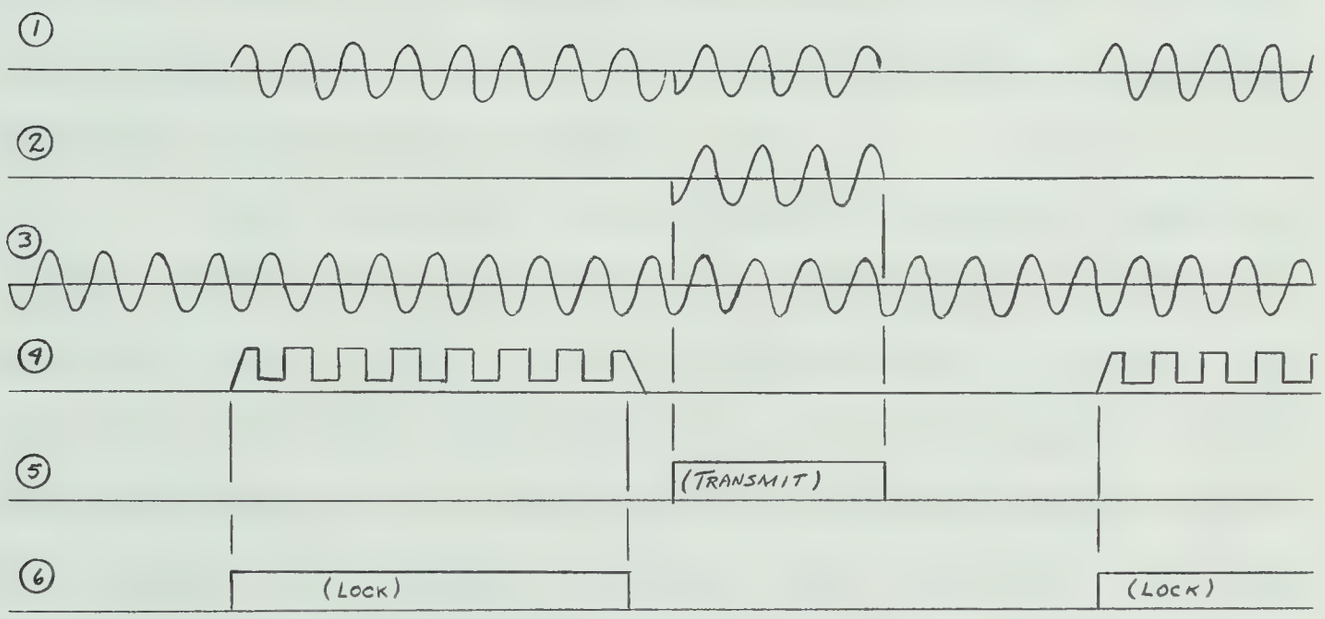

Fig. 3.4 Transponder Waveforms

3.2 The Observer's Station Operation

Referring to Fig. 3.1, the 10 KHz frequency is established by counting down a crystal controlled 100 KHz oscillator. The waveform of the oscillator is rich in harmonics and can be formed into a train of 2 1/2 microsecond wide pulses simply by applying it to a digital gate. A counter selects every tenth pulse and uses it to periodically reset an integrator whose input is a dc signal, and the result is a 10 KHz linear ramp. The same pulse locks a 10 KHz voltage controlled sine wave oscillator so that its zero crossings correspond to the fall of the pulse. This fall coincides with the start-up of the ramp, and is the time reference throughout the system, so that the width of the pulse only affects the unusable portion of the ramp, which is 2 1/2% of each cycle.

The train of 10 KHz pulses is counted down by a factor of 64 to establish the interrogation cycle (as distinct from a cycle of the 10 KHz signal). During one half of this period the observer's station transmits the 10 KHz sine wave via the operational amplifiers to the cable. The output of the gate driving the transistor in the feedback path of the OA3 operational amplifier (Sec. 4.1) is negative, turning the transistor off and permitting the amplifier to pass the signal from the oscillator. This sine

wave is transmitted by the OA4 operational amplifier down the cable to the transponder, which uses it to lock another oscillator.

During the second half of the interrogation cycle the receiver of the base station receives the transponder reply, if there is one. The transmitting OA3 is shorted by a saturated transistor during this half cycle and has no output. The OA4 has no drive and has very low output impedance, so the only signal on the cable is from the transponder. The digital circuit waits one cycle of the 10 KHz audio tone to let transients die away and then turns on the slow gate, which permits pulses from the receiver to trigger the sample-hold circuit.

The receiver consists of the second OA3 and a fast differential amplifier. The OA3 with its feedback diodes is a logarithmic amplifier which acts as an active zero crossing detector, with very high gain in the region of the input zero crossing. This OA3 drives a differential amplifier which makes a square wave of the signal, with a very fast fall corresponding to the zero crossing of the transponder response. This fall is differentiated by the input circuits to the sample-hold and causes it to sample the voltage on the ramp at this instant and hold it until the next sampling pulse.

Since the ramp begins at the observer's station

zero crossing and is sampled at the delayed transponder zero crossing the output of the sample-hold is proportional to travel time plus the system delays, which are nulled out. After seven cycles the slow gate is closed, giving a ramp at the output of the differential amplifier, which, when differentiated, does not cause a spurious sample to occur. The resulting voltage is held during the remainder of the interrogation cycle and displayed on a meter.

3.3 The Transponder Operation

The transponder normally is idle, with only its receiver operating. The waveform on the cable, whether it originates from the base station or the transponder's own transmitter, is formed by the Schmitt trigger into pulses. These are processed by the digital circuitry, which activates first the receiver and then the transmitter. From the end of the first cycle to the end of the thirty first cycle phase information is stored in the phase-locked oscillator. If the count stops at the end of the thirty second cycle, this phase information is returned to the observer's station by the transmitter in a 16 cycle burst. The transponder then returns to its receiver mode until it receives another train of exactly 32 cycles.

The receiver is an OA1 logarithmic amplifier

followed by a fast differential amplifier. The output square wave is differentiated, giving a 10 KHz train of very narrow pulses. These pulses occur at the zero crossings of the received signal, and act as an input to the phase-locked oscillator. When this oscillator has an input, it corrects its phase so that its zero crossings correspond to the pulses, and its zero crossings are then locked to those of the received signal. When it has no input the oscillator continues to oscillate in synchronism with the previous pulse train. The slow gate is made (by the digital circuits) to short circuit the pulses from the receiver except during the desired locking signal.

The transmitter consists of an OA4 and an OA3, which receives its input from the phase-locked oscillator. During the transmission period the transistor in the feedback path of the OA3 is cut off. During the rest of the interrogation cycle it is short circuited and the transmitter gives no output.

CHAPTER 4

DETAILS OF CIRCUITS

4.1 General

The circuits shown in block diagram form in Figs. 3.1 and 3.2 were constructed on boards and mounted in utility racks with interconnections made on the racks by spade leads. The racks had +12v and -12v well regulated power supplies.

The rack mounted equipment used two locally designed types of operational amplifiers, designated OA3 and OA4 (Ref. 8). The OA3 has an open loop gain of over 10,000 at low frequencies, about 600 ohms output impedance and a unity gain bandwidth of about 15 MHz. The OA4 has roughly the same open loop gain and bandwidth but has an output impedance of under 25 ohms and is capable of driving a 10 ohm load to 10 v peak. The OA1 is a very simple circuit stitch wired into the circuitry on the phase-locked oscillator boards, where it was chosen for compactness. The OA1 has an open loop gain of about 1200, a unity gain bandwidth of about 15 MHz and output impedance of 12 k. All three have an input impedance of 150 k.

Each rack had a general purpose digital patch board on which the digital circuitry to control the unit was set up. These boards are constructed with Motorola MC790

dual JK flip-flops, MC724 quad gates and MC799 dual buffers, which are mounted on a vector 812 plug-in patch board for easy interconnection.

4.2 The Crystal Controlled Oscillator

The 100 KHz reference oscillator circuit is shown in Fig. 4.1. The crystal operates inductively in its parallel mode at 99.95 KHz. The error is due in part to the class C operation and to the large values of C_1 and C_2 that were used for reliable pulse forming. The frequency drifted less than 210 ppm from -50 to +50 degrees C.

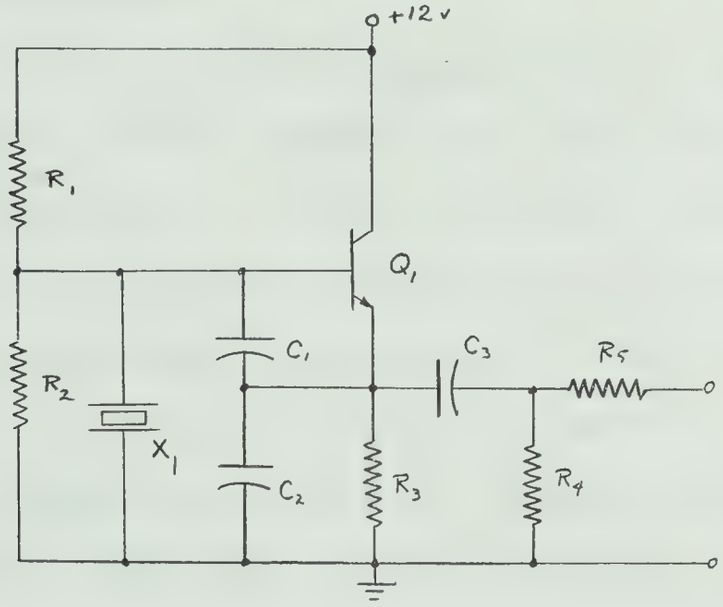

Fig. 4.1 Circuit Diagram of Oscillator

R_1--220k C_1--500pf Q_1--2N4401

R_2--820k C_2--680pf

R_3--10k C_3--1000pf

4.3 The Digital Circuits

4.3.1 Observer's Station Control Circuit

In Fig. 4.2 the upper four flip-flops are connected as a binary coded decimal counter to produce a 10 KHz pulse train. The ninth count permits resetting of the counter on the next pulse and enables an AND gate which passes this tenth pulse through to the ramp circuit and phase-locked oscillator. (The extra gates delay the pulses entering the AND gate to prevent resetting of the ramp by an extraneous spike which is caused by delay of the first count within the register.)

The output of this counter then toggles a six bit binary counter which counts to sixty four, giving the interrogation cycle. During the states from thirty two to sixty four the Q output of the last flip-flop is a logical 1 and the transmitter is activated. In the zero state the Q's of the last three flip-flops are all zero, and the Reset terminal of the lower flip-flop is enabled with a zero. The next fall of $\overline{Q}$ of the first flip-flop of the 64 state counter will cause the lower flip-flop to change state, and $\overline{Q}$ becomes zero, enabling the receiver for measurement of phase shift at the end of the first count. This one cycle delay is introduced to prevent errors due to transients when the transponder begins its transmission. When the count

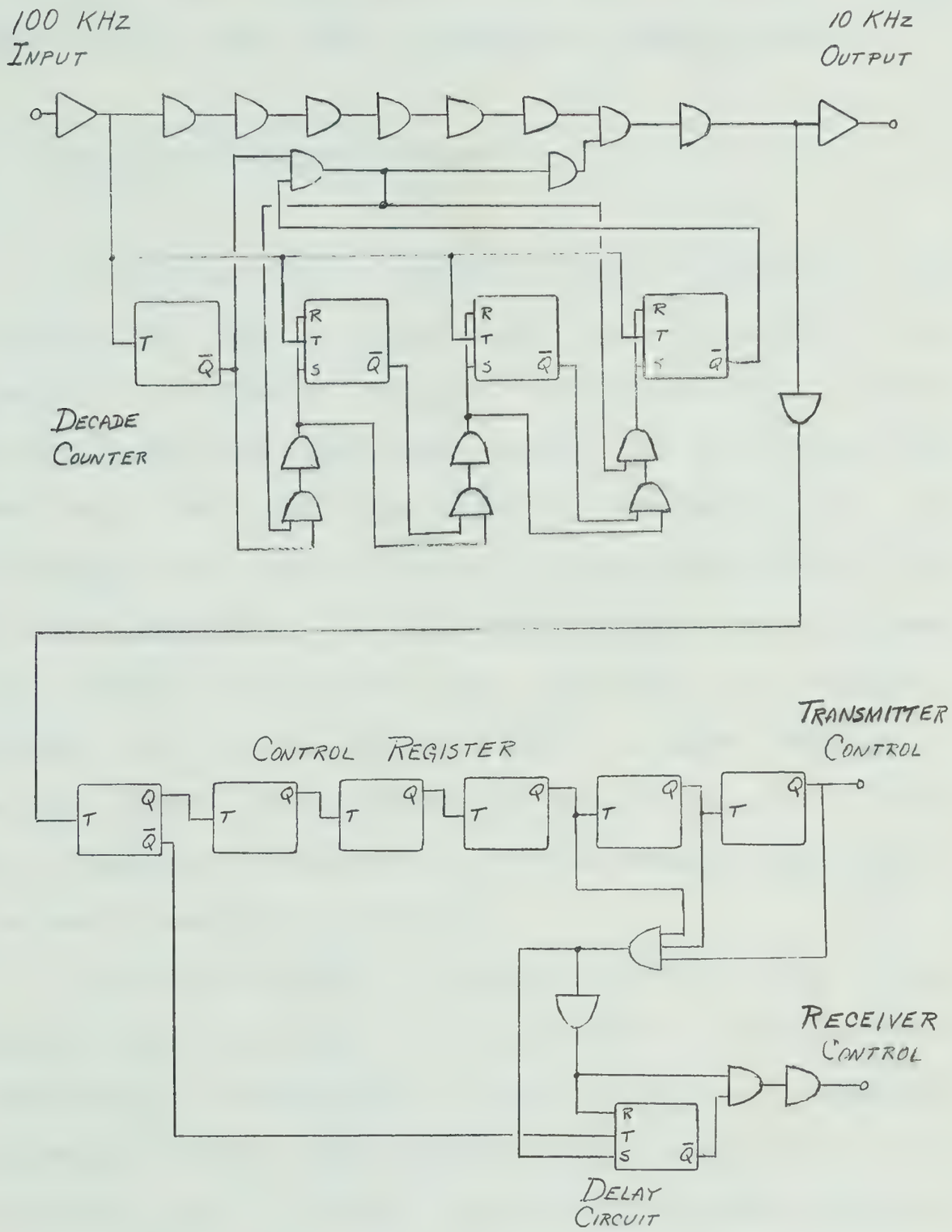

Fig. 4.2 Observer's Station Control Circuit

reaches eight the receiver is disabled and the count continues to 32, after which transmission begins again.

4.3.2 Transponder Control Circuit

On another digital board in the transponder rack the circuit of Fig. 4.3 was set up to control the transponder. A Schmitt trigger takes its input signal directly off the cable, and makes square pulses of both the received and the transmitted signals. It feeds a six bit binary counter and a gate which has a large capacitor on its output. This capacitor is discharged rapidly but charged much more slowly through the load resistor of the gate, which means that the following Schmitt trigger remains on during both tone bursts and doesn't change state until the signal on the cable disappears. It then presets the counter for the next interrogation burst.

After this Schmitt trigger falls on the first count an RS flip-flop (made from two gates) is set to zero and pulses begin entering the locking circuit. When the input Schmitt trigger falls on the thirty second cycle this RS flip-flop is set to one and the oscillator stops locking. The zero crossing occurs after the Schmitt trigger falls so transients from turnoff of the observer's station do not disturb the locking. The thirty second count is delayed by another gate with a capacitor on its output and sets another

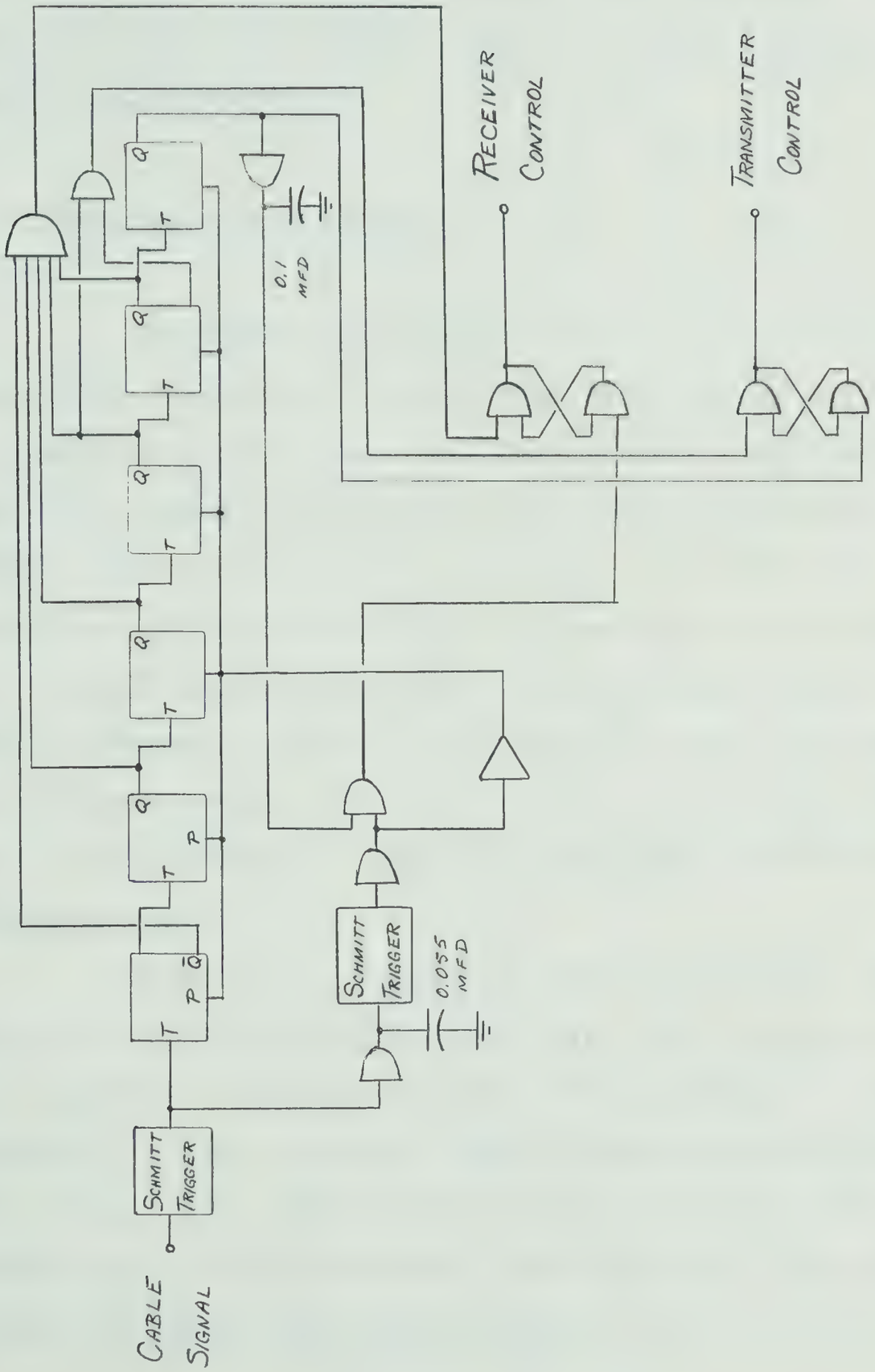

Fig. 4.3 Diagram of Transponder Control Circuit

RS flip-flop to its one state, which makes the transmitter return a 16 cycle tone burst. On the sixteenth cycle of any burst a reset pulse is applied to this flip-flop, ensuring that the transmitter never remains on continuously in the event of a malfunction.

4.4 The Sample-Hold Circuit

The sample-hold circuit of Fig. 4.4 is similar to the circuit described by MacFarlane (Ref. 9) and others. It is essentially the same as the standard OA3 operational amplifier with Q_7, Q_8, Q_9, and Q_{10} plus a hold capacitor C_1 added. The open loop gain is normally zero during the hold period and the output voltage is determined by the charge on C_1. During the sampling pulse the gain becomes about 20,000 and the feedback adjusts the output to equal the input (in the follower mode: Fig. 4.7), follows the output until the end of the aperture, and holds the last voltage present before turn-off.

With C_1 = 7 nanofarads the circuit can slew 10 volts in 1 1/2 microseconds; 200 nsec for turn-on, 300 nsec for settling and 1 microsecond for slewing at about 70 v/μsec nf. After turnoff the voltage sags 600 mv/sec nf. The slewing rate can be increased by increasing the current through Q_{13}, but it becomes more difficult to keep the circuit stable for as large a range of C_1. The output error

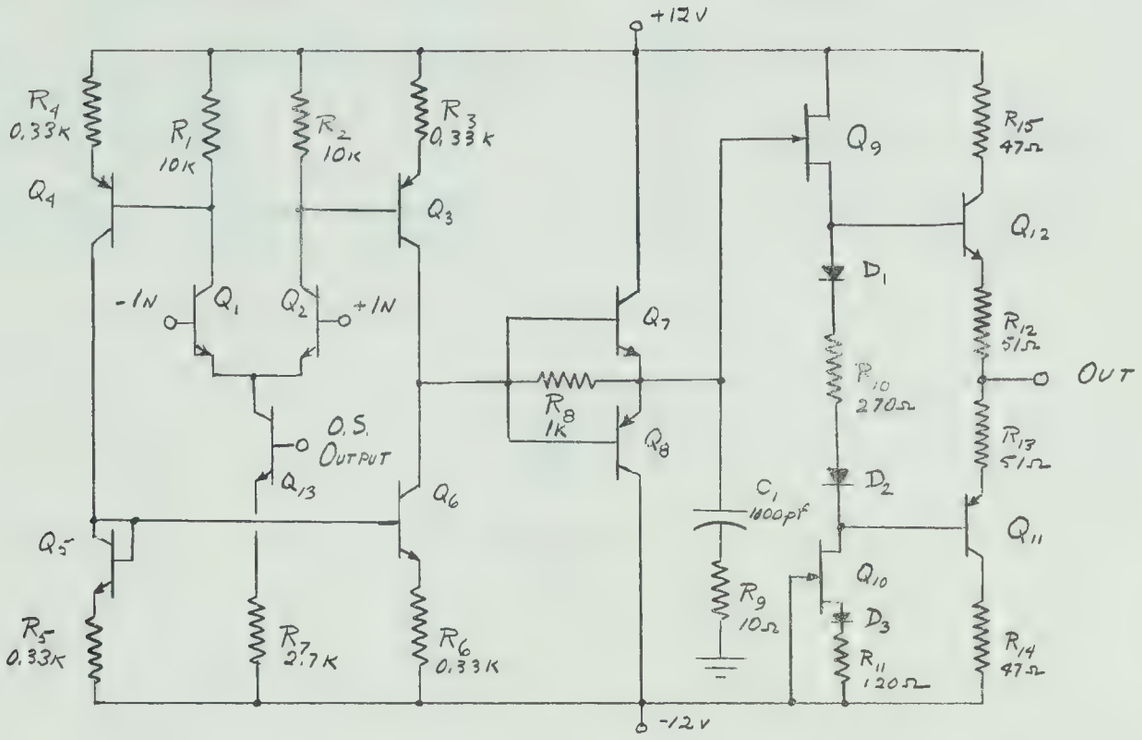

Fig. 4.4 The Sampling Circuit

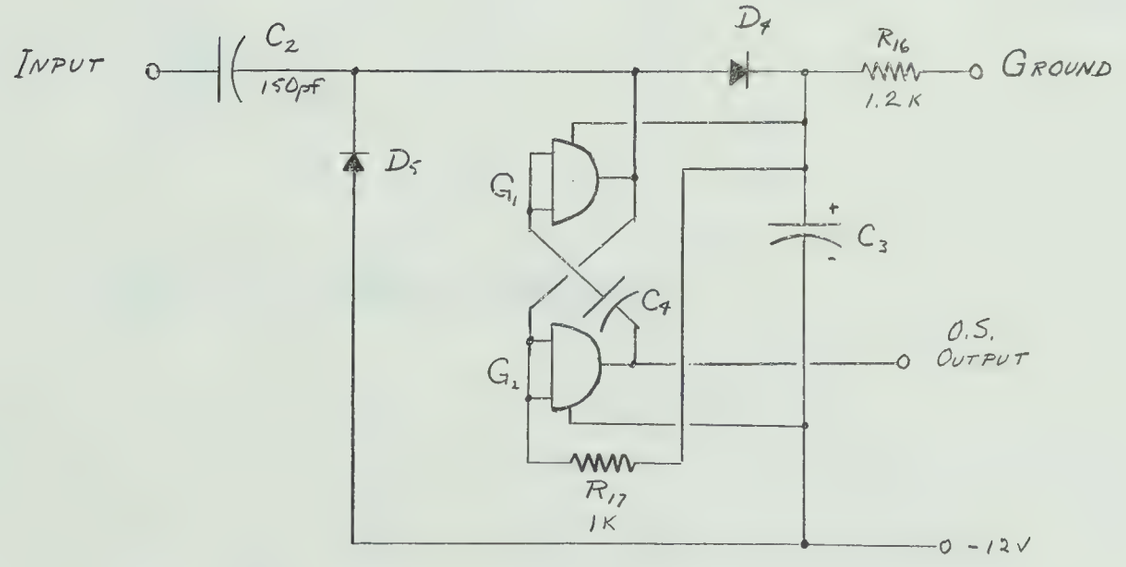

Fig. 4.5 The One-Shot Multivibrator

Q_1, Q_2 -- matched 2N3707

Q_3, Q_4, Q_8, Q_{11} -- 2N3906

Q_5, Q_6, Q_7, Q_{12} -- 2N3904

Q_9, Q_{10} -- selected 2N3819

Q_3 -- 2N3707

G_1, G_2 -- Gates in MC724

D_1, D_2, D_3 -- 1N456A

D_4, D_5 -- 1N3064

C_1 -- 1000 pf glass

C_2 -- 150 pf

C_3 -- 3.3 mfd Tantalum

C_4 -- 0.0025 mfd Mylar

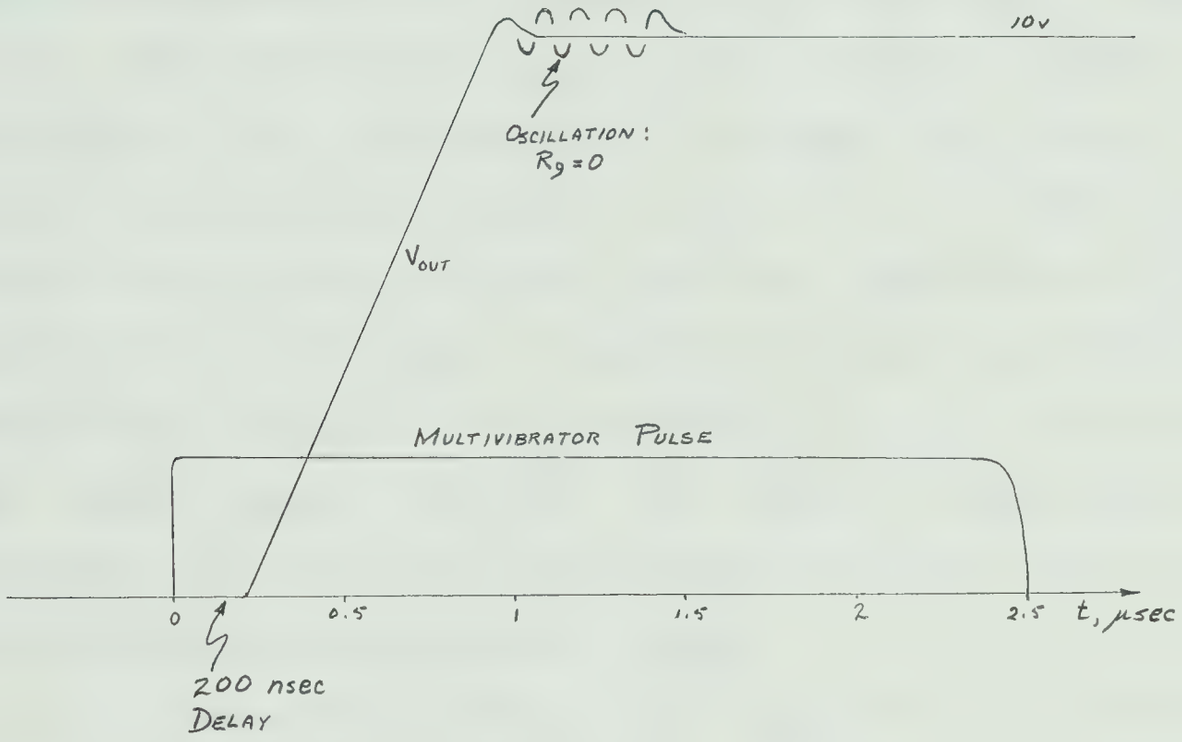

Fig. 4.6 Slewing Response

from sampling a DC signal was under 1 mv. The circuit will accept 12v between the bases of Q_1 and Q_2.

The sampling circuit is activated by a one-shot multivibrator whose output is applied between the base of Q_{13} and the -12v supply. Two of the four gates in a Motorola MC724 integrated circuit are connected as in Fig. 4.5. Varying C_4 permits adjustment of the pulse width. The effect of temperature on pulse width is tabulated in Table 4.1. The trip pulse must be very fast to trigger the circuit; in this application it triggers on a fall of 4 volts in 100 nsec, and rejects a fall of 8v in 600 nsec, which results from the use of the Miller capacitance in Fig. 4.11 on the slow gate. D_4 and D_5 prevent large incoming pulses from destroying the integrated circuit, by shunting the excess signal into the -12v supply or C_3. This was necessary since C_2 can be increased for other applications with an unpredictable range of inputs.

Returning to Fig. 4.4, Q_{13} acts as a current source, driving the differential input pair Q_1 and Q_2 and receiving its drive from the one-shot multivibrator output (Fig. 4.5). Q_4 is a unity gain inverter driving Q_6, acting in push-pull with Q_3 to drive R_8 and C_1. If the voltage across R_8 exceeds V_{be} of Q_7 or Q_8, the transistor conducts, increasing the available slewing current by its current gain, h_{FE}. When the current from Q_{13} is cut off, only leakage currents flow in Q_3, Q_6, Q_7 and Q_8, giving rise to

the sag during hold. These transistors were selected for low, matched I_{ces}. The stored charges should be the same, so complementary types were used. Q_9 is a source follower FET for minimum current drain from C_1 during the hold period. Q_{10} is a matched FET which gives a current source load for a gain closer to unity of Q_9. If R_{11} is set to 1/2 R_{10}, temperature changes in characteristics of the two FET's track and the voltage at the output remains constant to first order.

Following are three configurations that can be used:

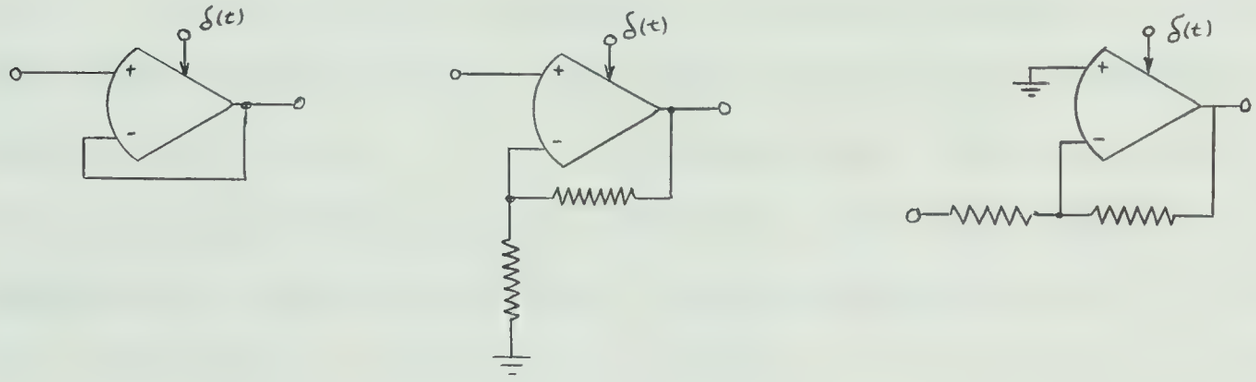

Follower Positive Gain Negative Gain

Fig 4.7 Some Configurations for the Sample-Hold

In the negative gain mode Q_1 or Q_2 can receive more than 12v and break down due to the possibility of the input going as much as 10 volts positive while the output is held as much as 10 volts negative. Breakdown causes the circuit to cease holding and follow the input with about 12 1/2 volts offset, the breakdown voltage of the avalanching transistor.

To prevent this it was decided to use the follower mode rather than putting diodes in the emitters of Q_1 and Q_2 (Ref. 10) with attendant matching problems.

During the aperture the circuit tended to oscillate with about 6 cycles of a high frequency, then die away (Fig. 4.6). The nonlinearity causing this type of oscillation is the hysteresis in Q_7 and Q_8. This oscillation was reduced to 1/2 cycle by adjusting R_9 to 10Ω.

4.5 The Ramp Generator

This circuit produces a voltage sawtooth which starts at zero volts at the zero crossing and increases linearly with time. It is discharged just before the next zero crossing. The ramp portion of the wave is produced by integrating a constant voltage during the time that Q_1 of Fig. 4.8 is off. When Q_1 is turned on by the reset pulse from the digital circuit (4.3.1) it becomes a low value of feedback resistor. The configuration is then a very low gain amplifier with nearly zero output. Current is fed back during the reset pulse from the output to the summing junction to cancel current from the base drive circuit, the constant input current and the discharge current from C_1. The transistor is able to remove the charge on C_1 in about 1/3 microsecond. The saturated voltage V of Q_1 is given in Table 4.1.

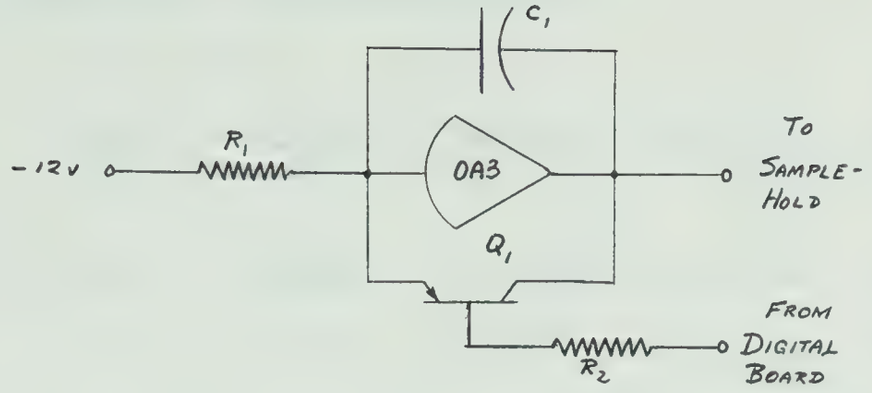

Fig. 4.8 Circuit Diagram of Ramp Generator

Component values are as follows:

R_1-- 6.32k metal film in series with 4.7k, Philips carbon. This was selected for temperature tracking and for proper slope of the ramp. The results of tests are shown in table 4.1.

C_1-- 0.01 mfd glass. The ramp was not linear for most other capacitors tried because of hysteresis in the dielectric.

Q_1-- 2N3704

R_2-- 8.2k

To check for temperature tracking the n'th pulse of the 100 KHz pulse train was selected by a four bit gate on the digital board and applied as a trip pulse to the multivibrator of the sample-hold circuit. The ramp was applied to the input and the output read by a DVM. The aperture width p was measured by an oscilloscope.

Table 4.1 Ramp Test Results

T°C	V_s, mv	Bit 0, v	Bit 2, v	Bit 9, v	p, μsec
-50	5.5	0.225*	2.326	10.140	2.52
-25	5.0	0.240	2.333	10.144	2.50
0	4.6	0.246	2.323	10.140	2.47
+25	4.4	0.242	2.316	10.161	2.45
+50	4.3	0.245	2.300	10.165	2.40

*It was later found that the supply had ~3v ripple.

The slope of the ramp was later decreased to give a reading of 10 mv per 100 ft of distance. In these tests the whole rack was put in the temperature controlled chamber and the errors combine power supply drift, ramp slope drift and aperture drift.

To check the ramp linearity, the voltages at the end of each of the ten pulses available from the digital board were compared against a voltage from a precision digital to analog converter. The pulse train was applied to the z axis of an oscilloscope and a multiple exposure photograph taken. The deviation was 0.04% or less. The circuit used and a sketch of the pertinent bright traces is shown in Figs. 4.9 and 4.10.

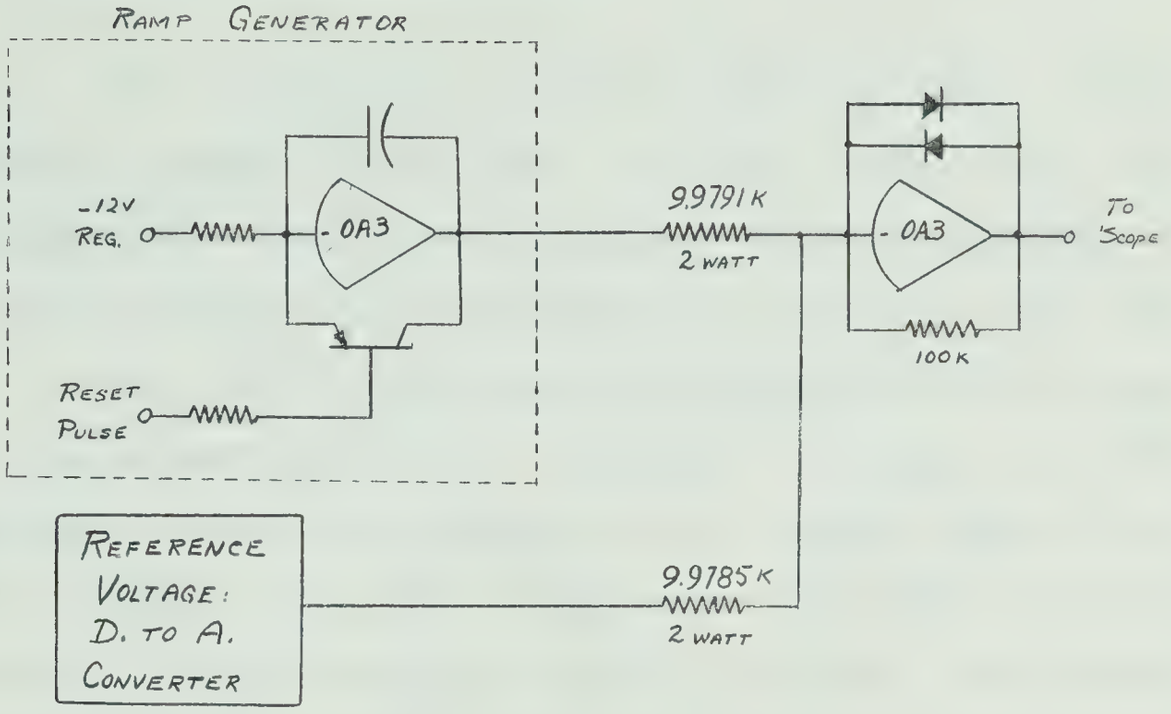

Fig. 4.9 Test Circuit for Ramp Linearity

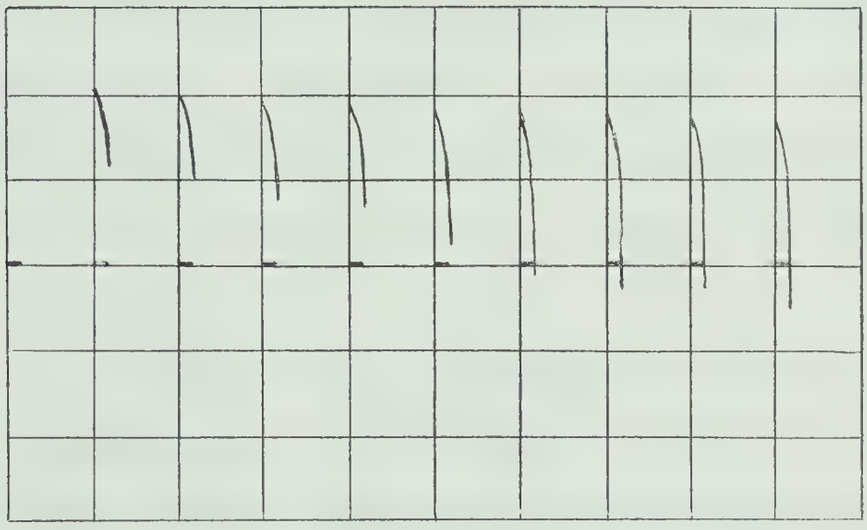

0.2v/div. Vertical 10 μsec/div Horizontal

Fig. 4.10 Bright Traces on Photograph

4.6 The Zero Crossing Detectors

The permissible system error was about twenty millivolts total, so this part of the system was quite critical. Referring to Fig. 4.11, a logarithmic amplifier was used to expand the zero crossing by 1200, the open loop gain of the OA1, before reaching the differential stage, which has a less predictable threshold of triggering. The logarithmic amplifier operates in its active region at all times, avoiding the slow response of saturated threshold detectors. In the region of the zero crossing the feedback current switches from one diode to the other as rapidly as the amplifier can respond. C_3 was added to reduce the mixing of RF interference with the 10 KHz signal.

The differential stage draws quite a heavy current to give a fast fall. This stage is designed to operate with infinite gain for speed but not as a Schmitt trigger to avoid offset and a large hysteresis loop. The differential gain is:

$$A_v = R_{11}/(h_{ib_1} + h_{ib_2}) = R_{11} I_e/\lambda \times (\alpha(1-\alpha))$$

Where I is the total current flowing into the emitters of Q_1 and Q_2 and α is the fraction of this that flows into Q_1. λ = 26 mv at room temperature. The feedback factor is given by:

$$G = h_{fe_2}(h_{ib_1} + h_{ib_2})/(R_3 + h_{fe_2}(h_{ib_1} + h_{ib_2}))$$
$$= 1 / (1 + R_3 I_e \alpha(1-\alpha)/h_{fe_2}\lambda)$$

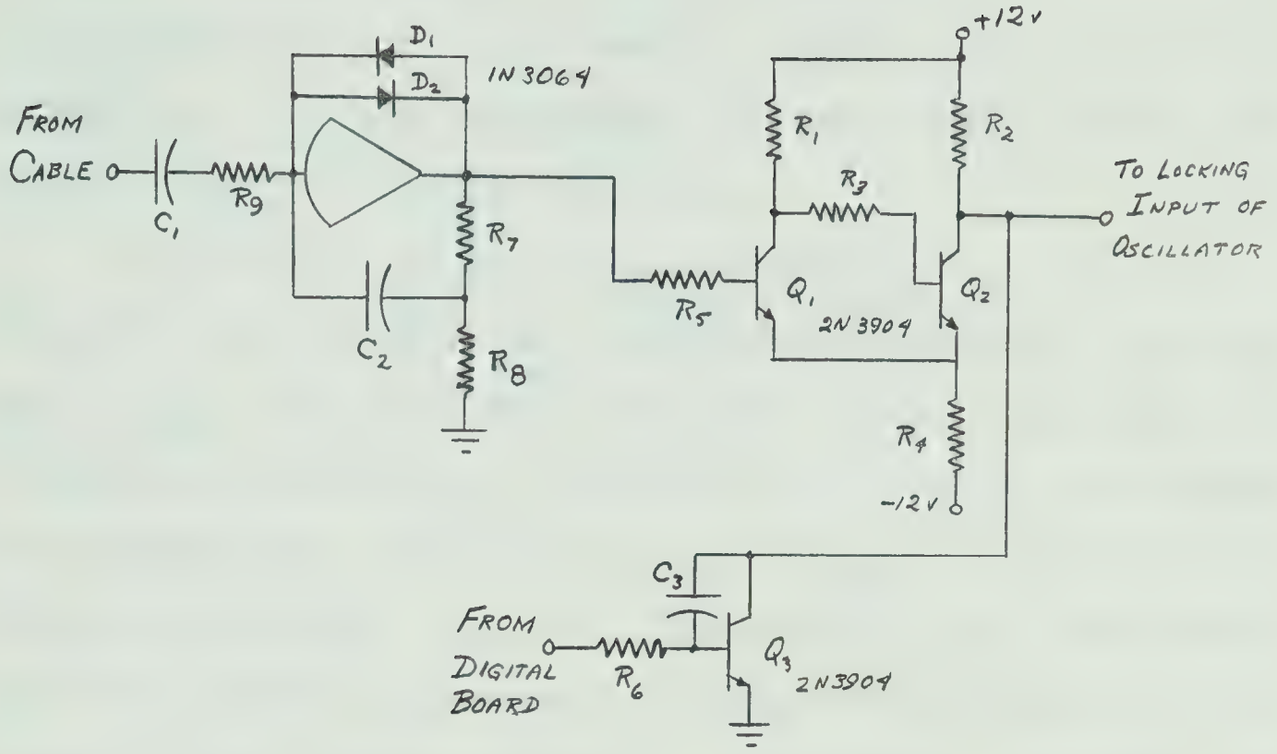

Fig. 4.11 Circuit Diagram of Zero Crossing Detectors

Observer's Station

R_1--0.68k	R_5--8.2k	R_9--2.2k	Q_1, Q_2, Q_3--2N3904
R_2--0.68k	R_6--10k	C_1--1mfd	D_1, D_2--1N3064
R_3--100k	R_7--Absent	C_2--Absent	A_1-- OA3
R_4--0.82k	R_8--Absent	C_3--Absent	

Transponder

R_1--1.8k	R_5--Absent	R_9--10k	Q_1, Q_2, Q_3--2N3904
R_2--1.8k	R_6--5.6k	C_1--0.1mfd	D_1, D_2--1N3064
R_3--220k	R_7--27k	C_2--15pf	A_1--OA1
R_4--2.2k	R_8--2.2k	C_3--50pf	

The product GA_v is given by:

$$GA_v = 1/((R_3/R_{11}h_{fe_2}) + (\lambda/R_{11}I_e\alpha(1-\alpha)))$$

The value of $\alpha(1-\alpha)$ is a maximum of 1/4 at $\alpha = 1/2$. The second term in the denominator is then 0.03 and we can write, using the binomial theorem:

$$GA_v = (R_{11}h_{fe}/R_3)(1 - h_{fe}\lambda/\alpha(1-\alpha)I_eR_3)$$

R_3 was chosen to make GA_v approximately unity for infinite gain. h_{fe} was assumed to be 150. This also puts the triggering threshold at zero volts if Q_1 and Q_2 are matched for base-emitter voltage and $h_{fe_2} = h_{FE_2}$. The hysteresis loop is infinitely narrow. Because of the logarithmic amplifier driving the circuit it works well even if R_3 is changed by a factor of two. Any attempt to speed up response with a capacitor in parallel with R_3 gives oscillation. The circuit used is shown in Fig. 4.10.

4.7 The Gated Amplifiers and Cable Drivers

To simulate a transmitter the circuit of Fig. 4.12 was used in both the transponder and the base station racks. The 0A3 operates at a gain of about 1/4 during its transmission time and during the receive portion of the cycle its measured gain was reduced by over 60 db. Blocking transmission is achieved by turning off Q_1, injecting into the base of Q_2, thus saturating it. The gain is then the ratio of its on resistance to R_1, and transmission is

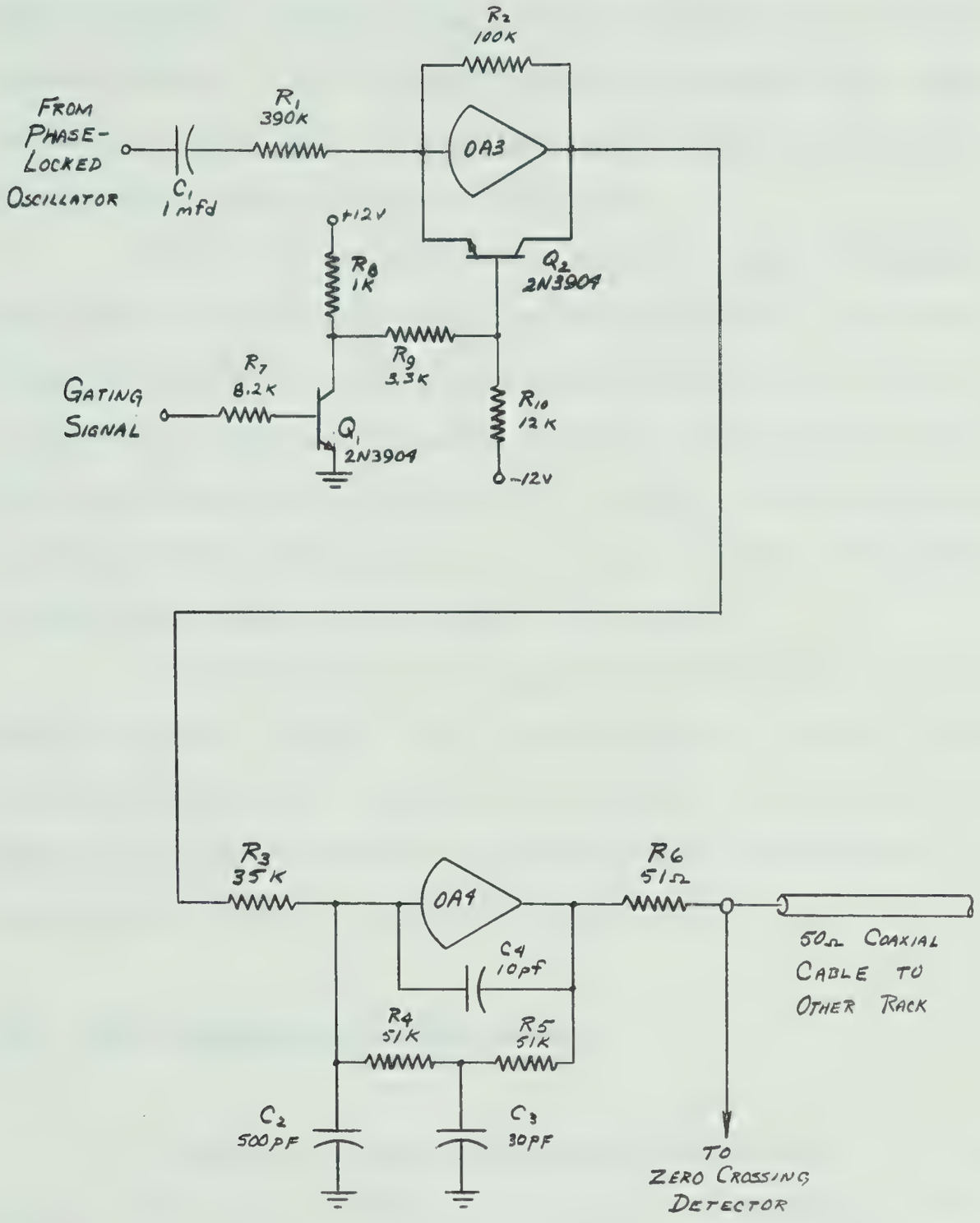

Fig. 4.12 Circuit Diagram of Gated Transmitter

prevented. To turn on the transmitter a positive voltage is applied to Q_1. This drives the base of Q_2 to -2.5 volts, and Q_2 does not affect the gain of the amplifier unless the output exceeds this voltage enough to forward bias the base collector junction of Q_2. This means that the circuit can accept more than 10 volts at the input.

The 0A4 cable driver has an output impedance of less than 10 milliohms when the feedback ratio is three, and the matching to the cable is accomplished by R_6 only. The bridged tee feedback network gives a bandwidth of 100 KHz with low phase shift at 10 KHz. The gain in the pass band is about three, bringing the voltages at the 0A4 output to 6v peak and those on the cable to 3v peak.

The base drive to Q_2 must be nulled out by the output current of the 0A3, resulting in a large turn-on transient when this current is suddenly cut off. For this reason and because of the transients at the beginning of a tone burst, the first zero crossing was not used.

4.8 The Phase-Locked Oscillators

The two phase-locked oscillators shown in Figs. 3.1 and 3.2 are 10 KHz sine wave oscillators with the circuit of Fig. 5.1. It will lock to any waveform within a few tenths of a percent of 10 KHz, providing that it has a rapid fall. The design of the phase-locked oscillator is

treated separately in Chapter 5 because of its importance in this transponder system.

CHAPTER 5

DESIGN OF THE PHASE-LOCKED OSCILLATORS

5.1 General

The phase-locked oscillator can be thought of as a servomechanism (See Fig. 5.6.). It accepts an input, which must have one rapid fall per cycle which is differentiated and formed into pulses. These act as the phase reference to a phase detector, whose other input is the output of a voltage variable oscillator. When the input frequency is within a few tenths of a percent of 10 KHz, the feedback effect of the loop corrects the phase of this oscillator until its negative going zero crossings are locked to the phase reference. In this case this is the pulse train corresponding to the zero crossings of the received signal.

Referring to Fig. 5.1, A_1 is a Wien bridge oscillator with C_1, C_2, R_1 and R_3 as frequency determining elements with voltage variable frequency control by Q_4 and adjustments R_2, R_4 and R_5. A_2 increases the slope of the zero crossing for more accurate locking (Appendix III). Q_6 passes the reference pulses to the phase detector, Q_5 which samples the output of A_2 and feeds the phase difference through the feedback network R_{13}, C_5 and C_8 to the gate of Q_4, completing the loop.

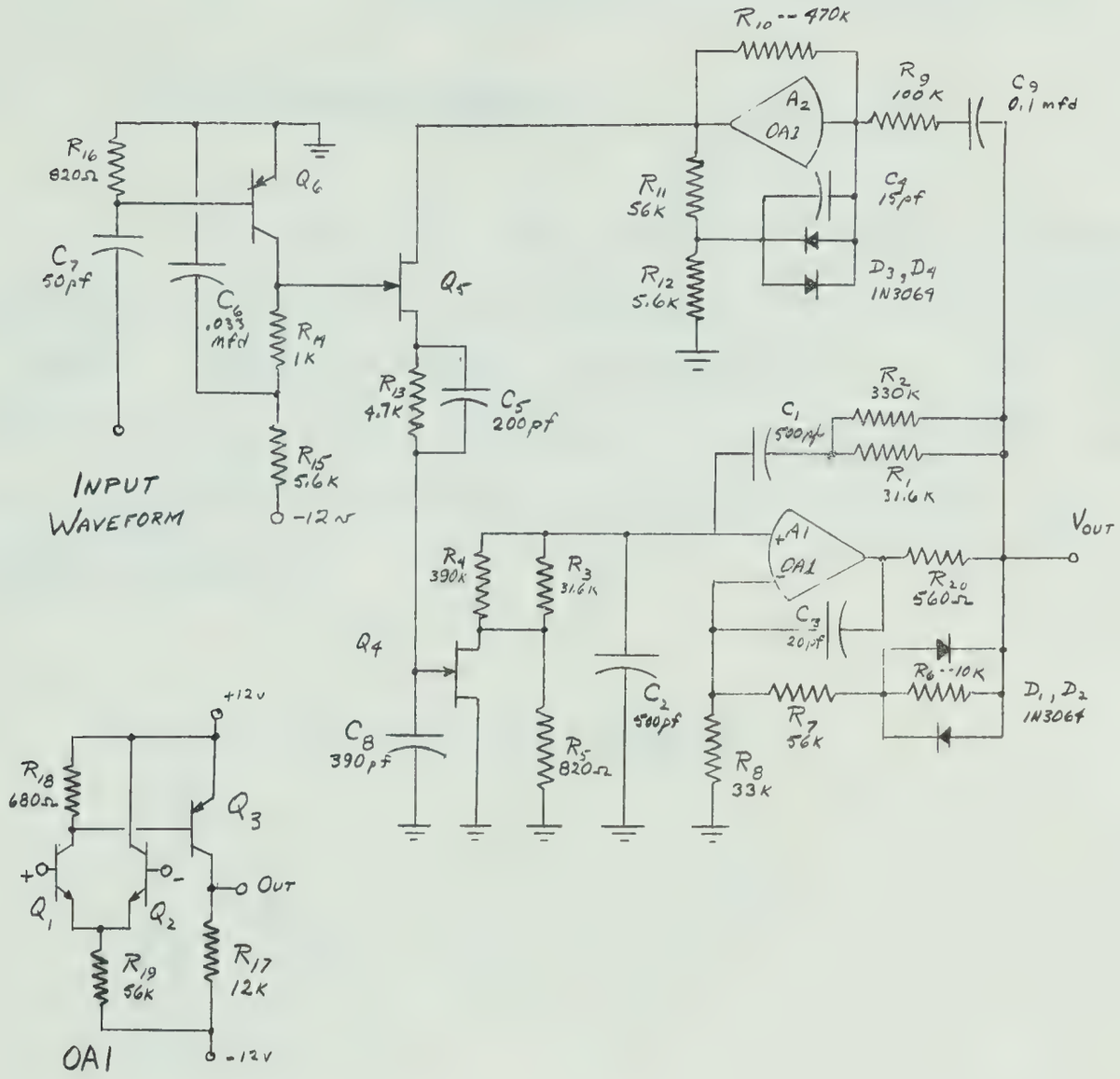

Fig. 5.1 Circuit Diagram of Oscillators

R_1, R_3--Metal Film C_1, C_2, C_3, C_7, C_8--Silvered Mica

C_6, C_9--Mylar

Q_1, Q_2--2N3707 Q_3--2N4058 Q_6--2N3906

Q_4, Q_5--2N3819, I_{DSS}= 2.5 ma., v_p= 1.2v

5.2 The Wien Bridge Oscillator and Lock Circuits

5.2.1 Frequency Control

In Fig. 5.2 the positive feedback network is assumed to consist of two identical resistors R, capacitors C and a voltage variable perturbation $r = \Delta R/R$, which needn't be positive. The amplifier with a positive gain G (its describing function) represents the OA1 with its feedback network.

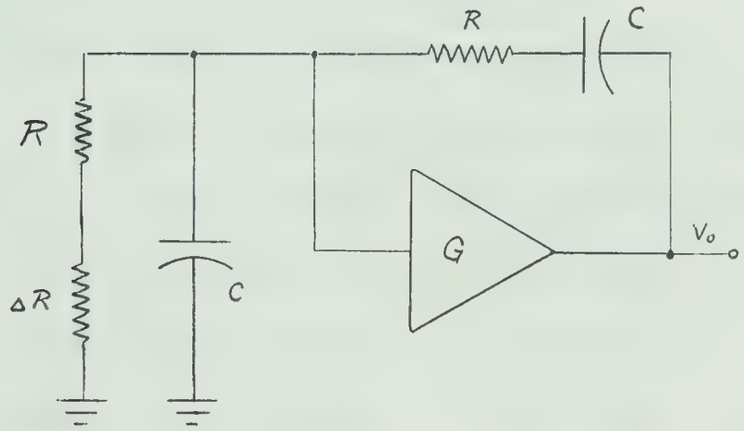

Fig. 5.2 Model of the Voltage Controlled Oscillator

The transfer function of the positive feedback network is:

$$H(p) = \frac{V_i(p)}{V_o(p)} = \frac{(1 + r)p}{1 + p(3 + 2r + r^2) + p^2(1 + r)}$$

where p = sRC, s being the Laplace transform variable. In the frequency domain

$$H(ju) = (1+r)/((3+r) + j\ \frac{(u^2(1+r) - 1)}{u})$$

If G is real, oscillation occurs for G = (3+r)/(1+r) and u= $1/(1+r)^{1/2}$. Changing r will slightly change the critical gain and will control the frequency as follows:

$$du/dr = -1/2(1+r)^{3/2}$$

At higher frequencies the magnitude of H(ju) drops and the phase lags. At lower frequencies the reverse occurs. The phase shift of H(ju) is given by:

$$du/dr = Tan^{-1}\ (u^2(1+r) - 1)/(3+r)u$$

The resistance perturbation is accomplished by Q_4, which is a field effect transistor operated in its triode region as a voltage variable resistor, with the gate voltage controlling the channel resistance and the drain voltage kept below 0.1v peak. The drain characteristics are described at low voltages by:

$$R_{DS} = R_o/(1-V_{GS}/V_p)^{1/2}$$

where R_o is the zero bias channel resistance, about 0.28k for the FET's used.

V_{GS} is the control voltage

V_p is the pinch-off voltage

Letting $r = R_{DS}/R$

$$\frac{dr}{dV_{GS}} = \frac{-R_o}{2RV_p}\ \frac{1}{(1 - V_{GS}/V_p)^{3/2}}$$

Using the chain rule our control function is:

$$K_o = \frac{du}{dV_{GS}} = \frac{-R_o}{4RV_p} \frac{1}{(1 - V_{GS}/V_p)^{3/2}} \frac{1}{(1+r)^{3/2}}$$

As can be seen this gives a very nonlinear control function. r is a function of V_{GS} with a 3/2 order pole at $V_{GS} = V_p$. At this voltage, u = 0. In the actual circuit, the amplitude rises and the output becomes a square wave of a low frequency. To limit the frequency deviation, R_5 was added in parallel with Q_4. This also linearizes the control function, and, as will be shown, increases loop stability and prevents noise from introducing locking error due to the curvature of the control function. Fig. 5.3 is an experimental plot of the control function with R_5 = 2.2k and 0.68k. Table 5.1 shows a check on the control range and temperature drift from -50 to +50 C.

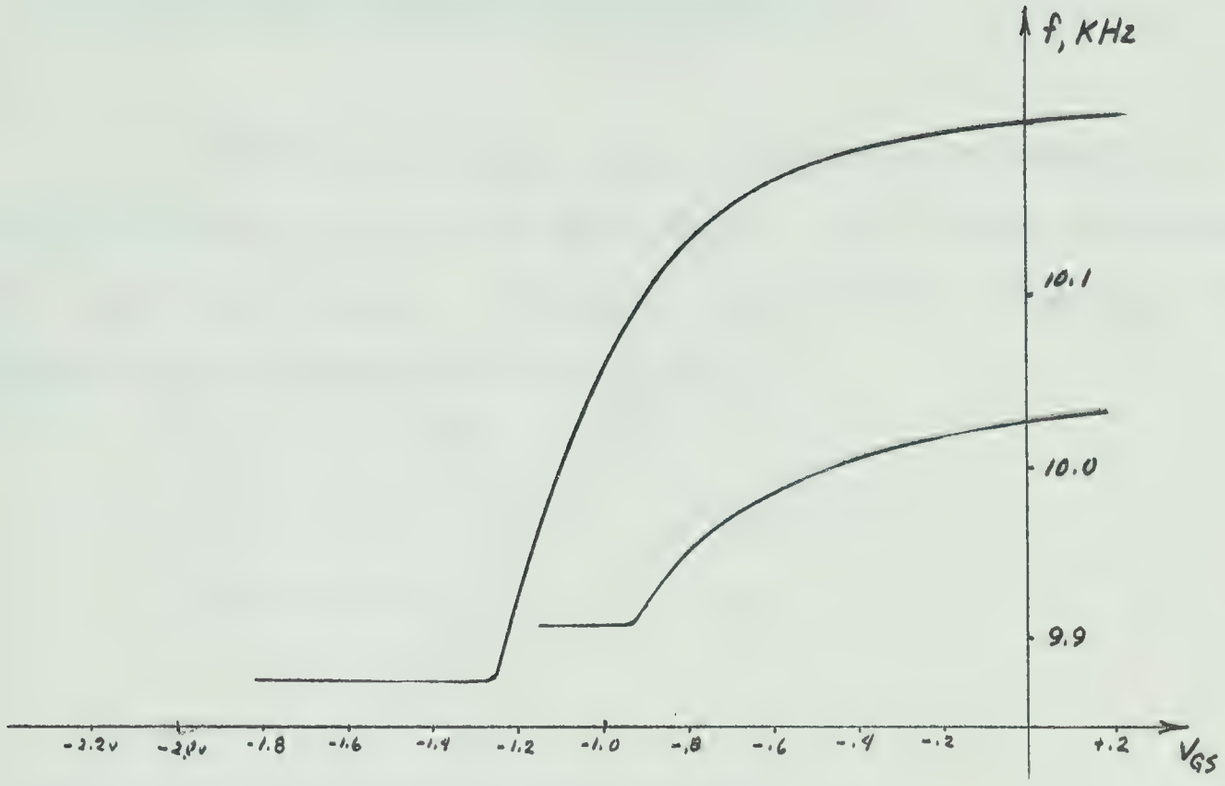

Fig. 5.3 Control Function of the Oscillator

Table 5.1 Control Range vs. Temperature

Temp.	Frequency	
T°C	FET Removed	FET Used, $V_g = 0$
-50	10.022	9.899
-25	10.030	9.9072
0	10.035	9.9052*
+25	10.048	9.9352
+50	10.057	9.9498

*The output was clipped, giving a frequency drop

5.2.2 The Positive Gain Amplifier

An OA1 was used in its positive gain mode with $G = (R_6+R_7+R_8)/R_8$ at low amplitudes. At higher amplitudes D_1 and D_2 conduct. Assuming zero diode resistance the dynamic gain becomes $G = (R_7+R_8)/R_8$.

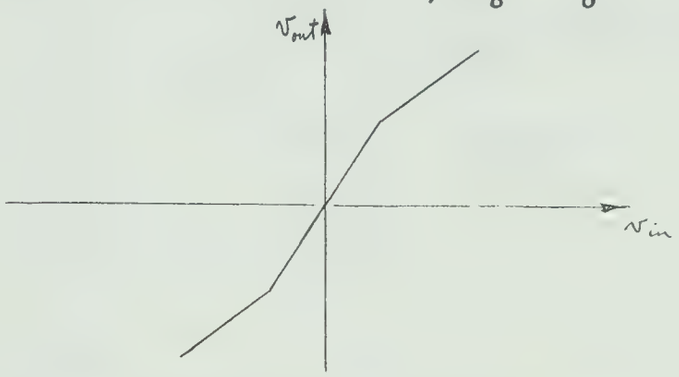

Fig. 5.4 Soft Limiting With Diodes

The knee of this transfer function is set at about 6 1/2 volts. The oscillation grows above this to the point that the describing function K_{eq} decreases to $(3+r)/(1+r)$, assuming that the frequency dependant network is a good filter. Since the limiting is 'soft' the distortion is low; 1.5% measured at 10v peak, and is mainly third harmonic, which doesn't affect zero crossings unless its phase is shifted (Appendix IV). It can be seen that K_{eq} must change with r,and as a result the desired frequency changes are accompanied by amplitude changes.

5.2.3 Effect of Amplifier Input and Output Impedances

Consider the positive gain amplifier in the Wien Bridge:

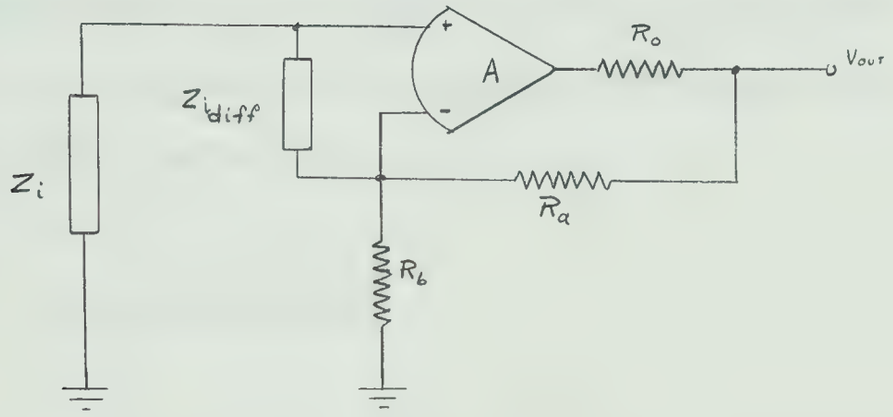

Fig. 5.5 Model of the Positive Gain Amplifier

The input and output impedances of this circuit are given by:

Z_o = R_a+R_b in parallel with $R_o/(1+AR_b/(R_a+R_b))$

Z_i' = Z_i in parallel with $Z_{i_{diff}}(1+AR_b/(R_a+R_b))$

Where R_o, $Z_{i_{diff}}$, A and Z_i are properties of the amplifier.

For the OA1 circuit of Fig. 5.1,

$Z_i = h_{ob_o} + j\omega C_{ob}$ of a 2N3707

$Z_{i_{diff}}$ = 140k in parallel with 28.6 pf.

A = 1000, Z_o = 12k

$AR_b/(R_a+R_b)$ = 300

Then Z_o' = 40Ω.

Z_i' = 2.5 pf in parallel with 15 megohms.

These have less than 1/2 % of the controlling effect of the frequency controlling elements. The temperature coefficients of semiconductor depletion capacitances were typically +100ppm/^{o}C, R_1 and R_3 varied - 11ppm/^{o}C and C_1 and C_2 varied +48ppm/^{o}C. One would expect a frequency shift of -37ppm/^{o}C. Looking at Table 5.1 it is +51ppm/^{o}C. It appears that A is not real as was assumed and phase lag increased as temperatures were lowered.

5.2.4 RF Interference

R_{20} and C_3 were added to prevent high frequency oscillation and to reduce RF interference from the transmitter (Appendix 1). Connecting this transmitter to the Wien bridge oscillator caused its frequency to shift by 0.09%. Since this occurs during the response interval of the transponder, it will cause an error. The loading effect of this circuit with the RF disabled was 0.025%. The error before the addition of R_{20} and C_3 to the circuit was 0.29%. Doubling C_3 caused no further improvement.

5.2.5 The Feedback Amplifier

A_2 in Fig. 5.1 operates as a linear amplifier over about ±6volts of its active range.The output is limited by

the feedback network, R_{11}, R_{12}, D_3 and D_4 at larger voltages to keep the amplifier in its active range. This amplifier increases the slope of the zero crossing by a factor of 4.7 and C_9 serves to reject DC offset in the Wien bridge. A small capacitor across D_3 and D_4 prevents RF interference from causing the diodes to conduct during the zero crossings.

5.2.6 The Pulse Generator

The phase reference to the oscillator is the output from a gate in the observer's station and from a zero crossing detector in the transponder. C_7 and R_{16} differentiate the input, and Q_6 is driven by the resulting waveform. The output at the collector of Q_6 is a very short sampling pulse. (In the observer's station C_7 is increased to 300 pf and fed by a 100 ohm resistor to accomodate the much faster rise time and lower voltage of the digital circuits.) During the sampling pulse the collector of Q_6 rises from -12v to 0v in 14 nsec, holds for 100 nsec, during which time Q_4 is conducting, and falls in 50 nsec. C_7 is silvered mica to make this width more temperature stable. The current drawn is 12 ma, which means that sharp spikes would be induced in the rest of the circuits unless R_{15} and C_6 are used as a filter. Because of the 0.1% duty cycle C_6 supplies almost all the current in a pulse.

5.2.7 The Phase Detector

Several phase detectors were considered, including the sample-hold circuit shown in Fig. 5.1 and the commonly used diode phase detector (Ref. 10). The noise performance of these detectors is discussed in Appendix 11. The sample-hold circuit takes a sample of the oscillator voltage at the zero crossing. This results in a voltage proportional to the phase difference between the two signals without large AC components. The diode detector passes the oscillator voltage during a large fraction of the cycle. This means that large AC components are present and must be filtered out of the signal to prevent distance errors due to the nonlinearity of the control function of the oscillator (Fig. 5.3). This filter will slow down the locking time of the oscillator.

The diode phase detector is capable of filtering out high frequency noise (Fig. A2.3), and even order harmonics. However, the filtering action of the loop will confine the output noise to a band, centered on 10 KHz, about 2 to 4 KHz wide (Sec. 5.3). Since the first zero of Fig. A2.3 is at 20 KHz this detector will be of little additional help.

The output of the phase detector must be held on the oscillator during the return transmission, so the

sample-hold circuit is needed anyway.

For these reasons and its small size it was decided to use the sample-hold phase detector.

5.3 The Phase-Locked Loop

5.3.1 Analysis

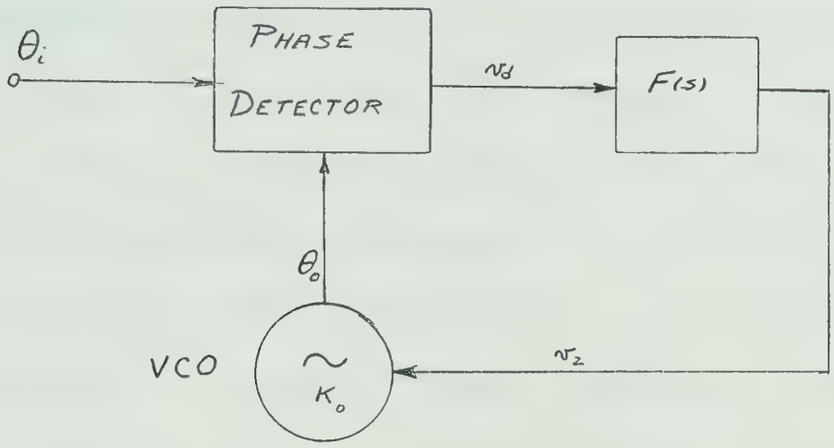

Fig. 5.6 Diagram of the Phase-Locked Loop

Following Gardner (Ref. 10) the phase detector output is proportional to the phase difference between inputs:

$$V_d = k_d(\theta_i - \theta_o)$$

The frequency deviation of the VCO (voltage controlled oscillator) is given by:

$$\omega - \omega' = \Delta\omega = d\theta_o/dt = k_o v_2$$

where ω' is the frequency at 0v input.

Taking Laplace transforms,

$$\theta_o(s) = k_o v_2(s)/s$$

Analysing the loop,

$$\theta_o(s)/\theta_i(s) = H(s) = k_o k_d F(s)/(s+k_o k_d F(s))$$

The phase error is given by:

$$\theta_e(s)/\theta_i(s) = (\theta_i(s)-\theta_o(s))/\theta_o(s)$$
$$= s/(s + k_o k_d F(s))$$

The phase detector in this circuit is Q_5 of Fig. 5.1, receiving narrow pulses at its gate, and passing the output of the feedback amplifier through the filter network R_{13}, C_5 and C_8 during the pulse. This FET operates as a source follower during the pulse. It operates in its triode region and can accept about -0.65v to + 1.2v at the drain. (During slew-in large voltages appear on the drain, and Q_5 does not operate in its triode region. Positive voltages cause slewing in the pentode region, while negative voltages give gate current from the logarithmic amplifier, which R_{17} limits to 1 ma. The loop will lock well in either case.)

Q_5 passes a pulse amplitude modulated current wave into R_{13} and C_5. Let i_d be its low frequency component. Then

$$i_d = (t/T_o)(1/R_{DS})(A\, dv_o/d\theta\big|_{\theta_i-\theta_o} \quad (\theta_i - \theta_o) - v_d)$$

Where t is the pulse width, T_o is the period, A is the gain of the feedback amplifier and R_{DS} is the resistance of Q_5. Now combining the sampling function and the triode resistance of Q_5, ie.

$$(Adv_o/d\theta\big|_{\theta_i-\theta_o} \quad (\theta_i - \theta_o) - v_d) = i_d\,(T_o/t)R_{DS}$$

Let $v_o = V_o \sin\theta(t)$

$$dv_o/d\theta|_{\theta_i-\theta_o} = V_o \cos((\theta_i - \theta_o)t)$$

In the neighbourhood of the zero crossing this slope is V_o. Substituting,

$$v_d = AV_o(\theta_i-\theta_o)$$

and $$k_o = AV_o$$

The circuit representing F(s) is:

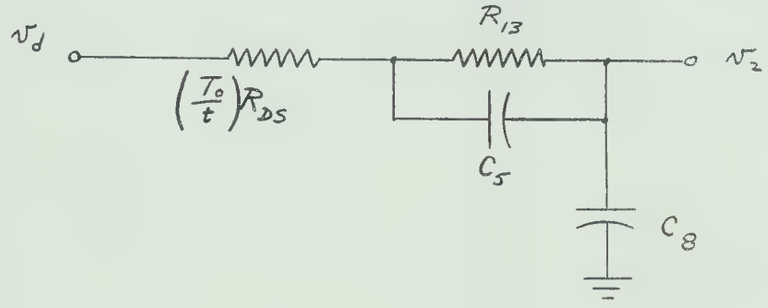

$$F(s) = (1+sR_{13}C_5)\Big/(1+sC_8[(T_o/t)R_{DS}]+s^2C_5C_8R_{13}(T_o/t)R_{DS})$$

Writing the error in the form

$$\theta_e(s)/\theta_o(s) = G(s)/(1+ G(s)H(s))$$

for construction of polar plots:

$$\theta_e(s)/\theta_i(s) = 1/(1+(1/s)k_ok_dF(s))$$

$$=1\Big/(1+(1/s)k_ok_d\frac{(1+sR_{13}C_5)}{(1+sC_8\{(T_o/t)R_{DS}+R_{13}\}+ s^2C_8C_5R_{13}\frac{T_o}{t}R_{DS})}$$

With $C_5 = 0$:

$$\theta_e(s)/\theta_i(s) = 1\Big/(1+k_ok_d/s(1+sC_8(T_o/t)R_{DS}+R_{13})$$

$$G(j\omega)H(j\omega) = k_ok_d\Big/j\omega(1+j\omega C_8((T_o/t)R_{DS}+R_{13})$$

Sketches of the polar plots of this function and that with $C_5 \neq 0$ are shown in Fig. 5.7.

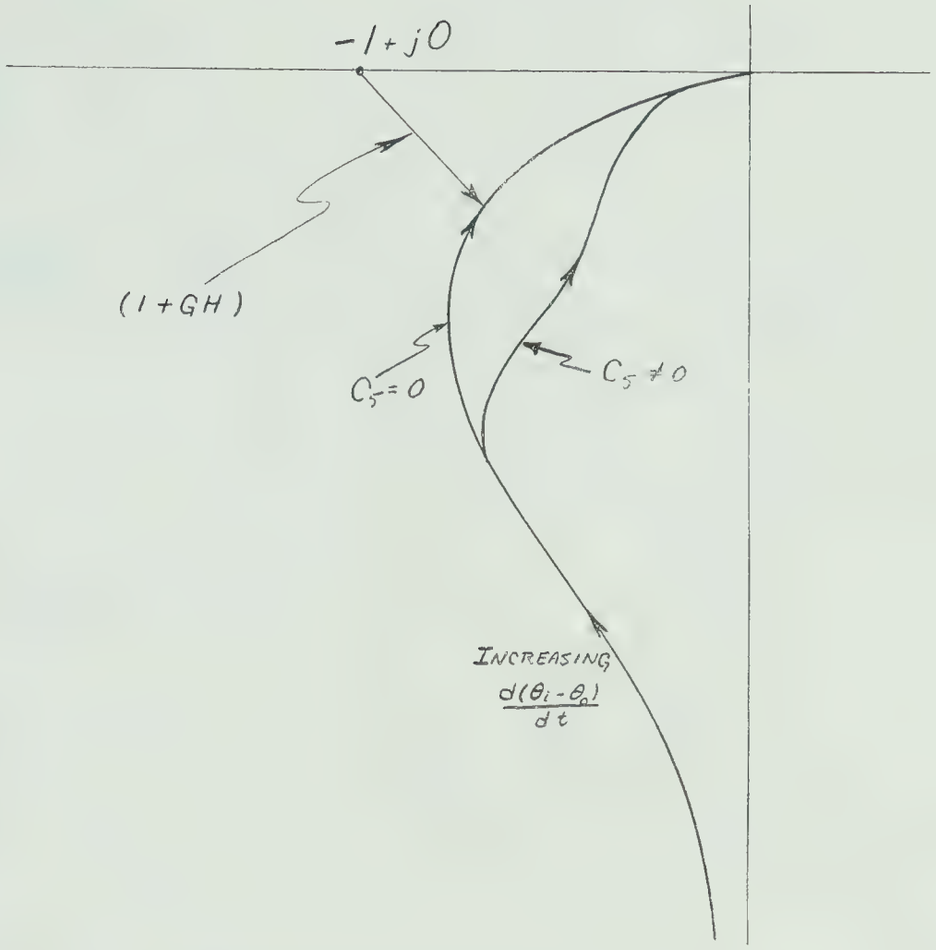

Fig. 5.7 Polar Plot of Loop Gain

Increasing the gain increases the denominator, and increases the peak of the error function, as shown in Fig. 5.8. C_5 can be selected so that this peak is almost removed for noise rejection. At the same time the speed of phase correction is improved.

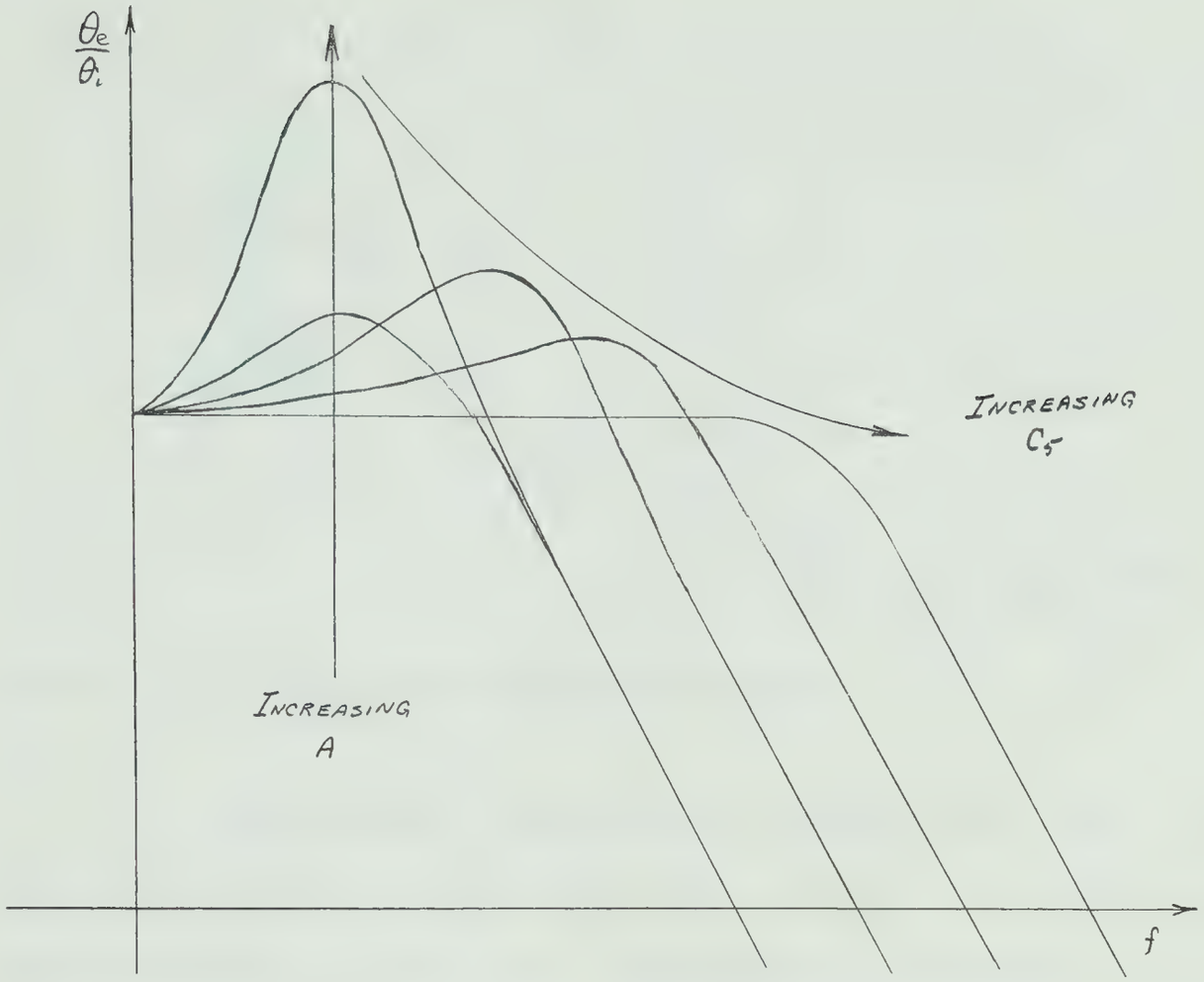

Fig. 5.8 Sketch of Phase Error Gain vs. Frequency

5.3.2 Transient Response Test of the Loop

The loop impulse response was used to select C_5 and C_8 for best settling time and minimum overshoot. Charge pulses were injected into C_8 and removed by the action of the loop. The circuit used is shown in Fig. 5.9.

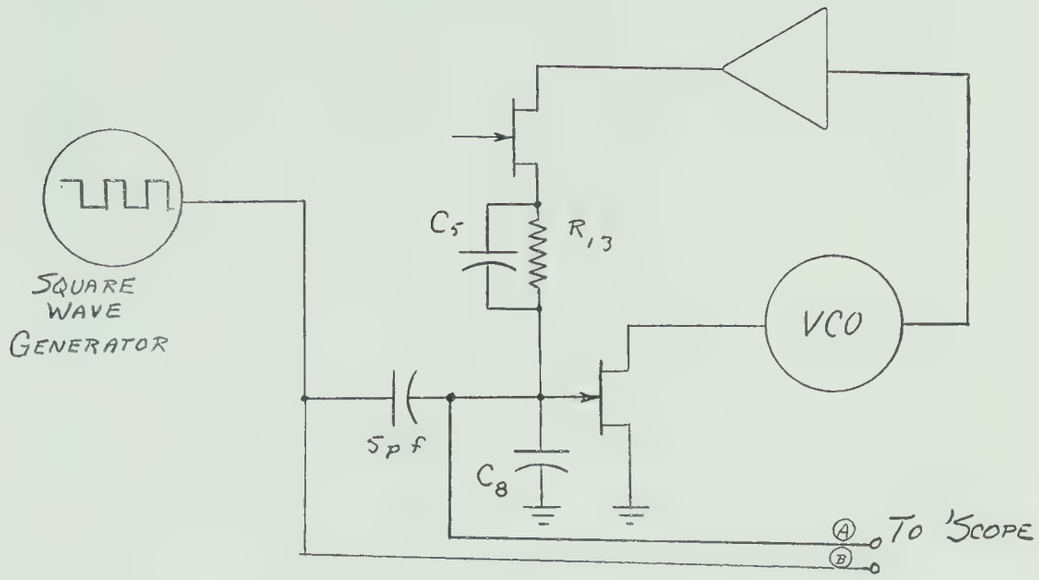

Fig. 5.9 Impulse Response Test Setup

Some results are shown in Figs. 5.10 and 5.11. Note the effect of nonlinearities in Fig. 5.11. This would cause distance errors in the presence of noise. R_5 was reduced to decrease nonlinearity in k_o (Fig. 5.3). R_{DS} is greater for positive error than for negative error, giving longer settling time.

In the above analysis the loop is unconditionally stable. In practice, it was not. At sufficiently high gain in the feedback amplifier, the loop oscillates, probably due to the finite response time of the sampling FET, which would make the equivalent body resistance a function of frequency, and the loop has order higher than two. The gain of A_2 was reduced and C_5 and R_{13} added to prevent this as well as to reduce the peak in noise response. Changing the sampling pulse width had only a minor effect.

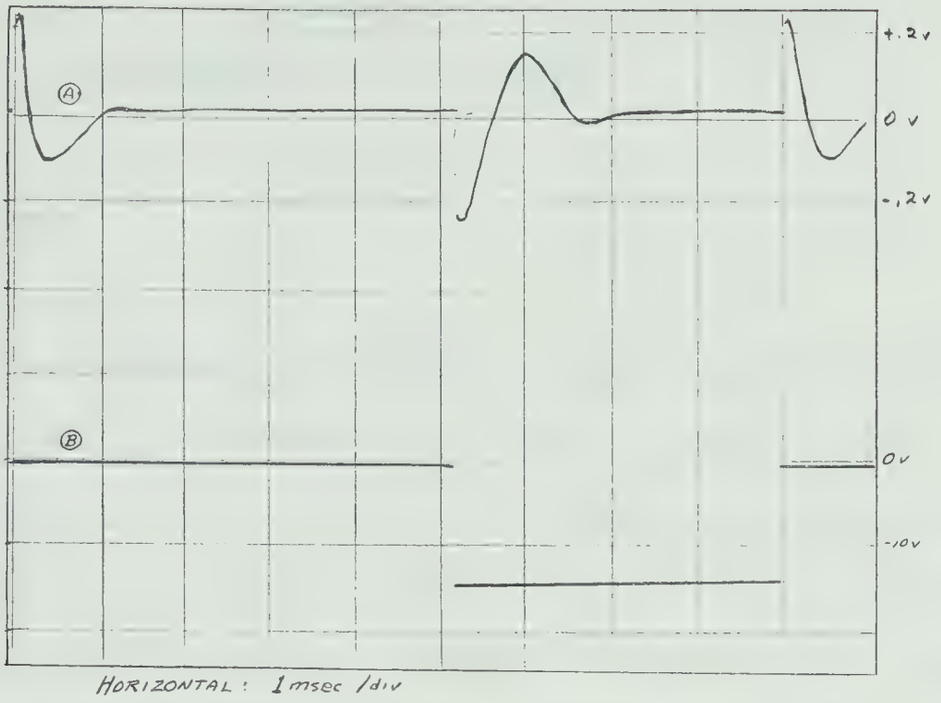

Fig. 5.10 Impulse Response, $v_g \doteq 0$

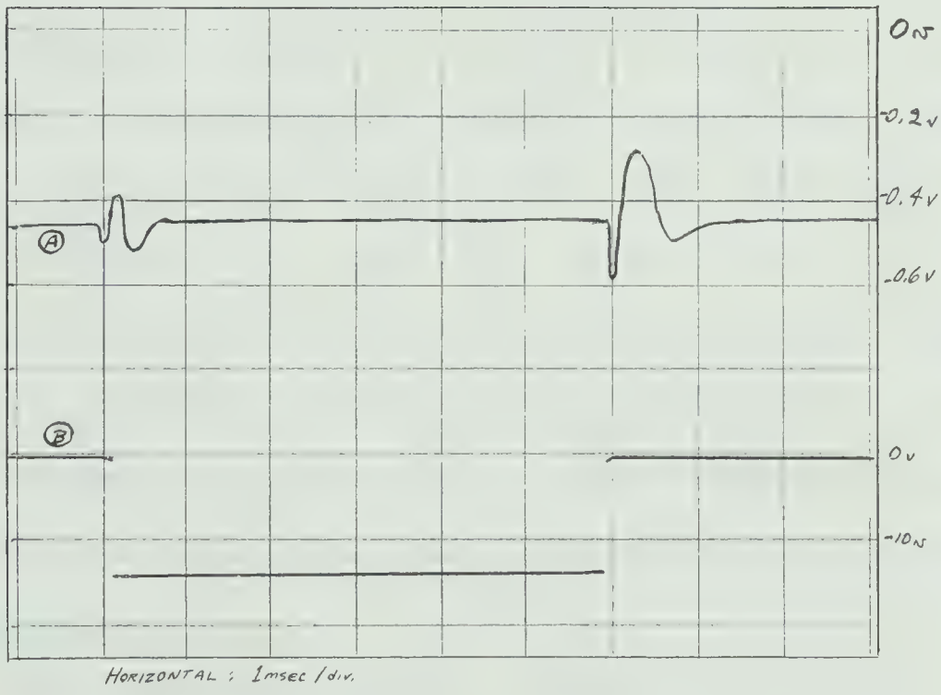

Fig. 5.11 Impulse Response, $v_g \doteq -1/2v$

CHAPTER 6

PERFORMANCE OF THE SYSTEM

6.1 General

The system was tested by measuring the length of a long cable and its length with a short cable added. The phase-locked oscillator board and the ramp generator and sample-hold circuits were tested for temperature drift in a Delta Designs environmental chamber. The output voltage was measured by a precision digital voltmeter for these tests.

6.2 Results

The short cable was found by measurement with a time domain reflectometer to have an electrical length of 68.6 feet. When it was added to the long cable the system measurement agreed with this to within 1/10 of a foot. Without the long cable there was an error of -10 feet, likely due to turnoff problems in Q_1 and dielectric problems in C_1 of the ramp generator (Fig. 4.8). The long cable was roughly 1500 feet long, too long to be measured by the time domain reflectometer.

The ramp generator and sample-hold circuits had a 75 foot error from $-50^{o}C$ to $+50^{o}C$ measured at the beginning of the ramp or at zero distance. The additional error due

to change of slope of the ramp was 0.25% (125 feet at full distance). The phase-locked oscillator board with its zero crossing detector had an error of 90 feet or 0.18% from -50°C to +25°C and an anomalous error of 680 feet at +50°C.

The effects of power supply variations on this board were measured and appear in Fig. 6.1. In this plot the supplies were varied independently. When they were varied simultaneously it was found that the effects of these variations on the output were independent. The errors depicted by this graph are of the order of 1/2 mile and a regulator should be used.

When the input signal to the transponder was mixed with 20 KHz band limited white noise the transponder retained lock with a signal to noise ratio as low as one. The RMS signal was measured by an oscilloscope and the noise by an RMS reading voltmeter.

6.3 The Final System

The final system can be built as in the test system with the substitution of transmitters for the OA4's and the addition of receivers to drive the zero crossing detectors. The digital circuit in the transponder should be replaced by a one-shot multivibrator scheme for less power drain and bulk.

The power to the transponder circuit, except for

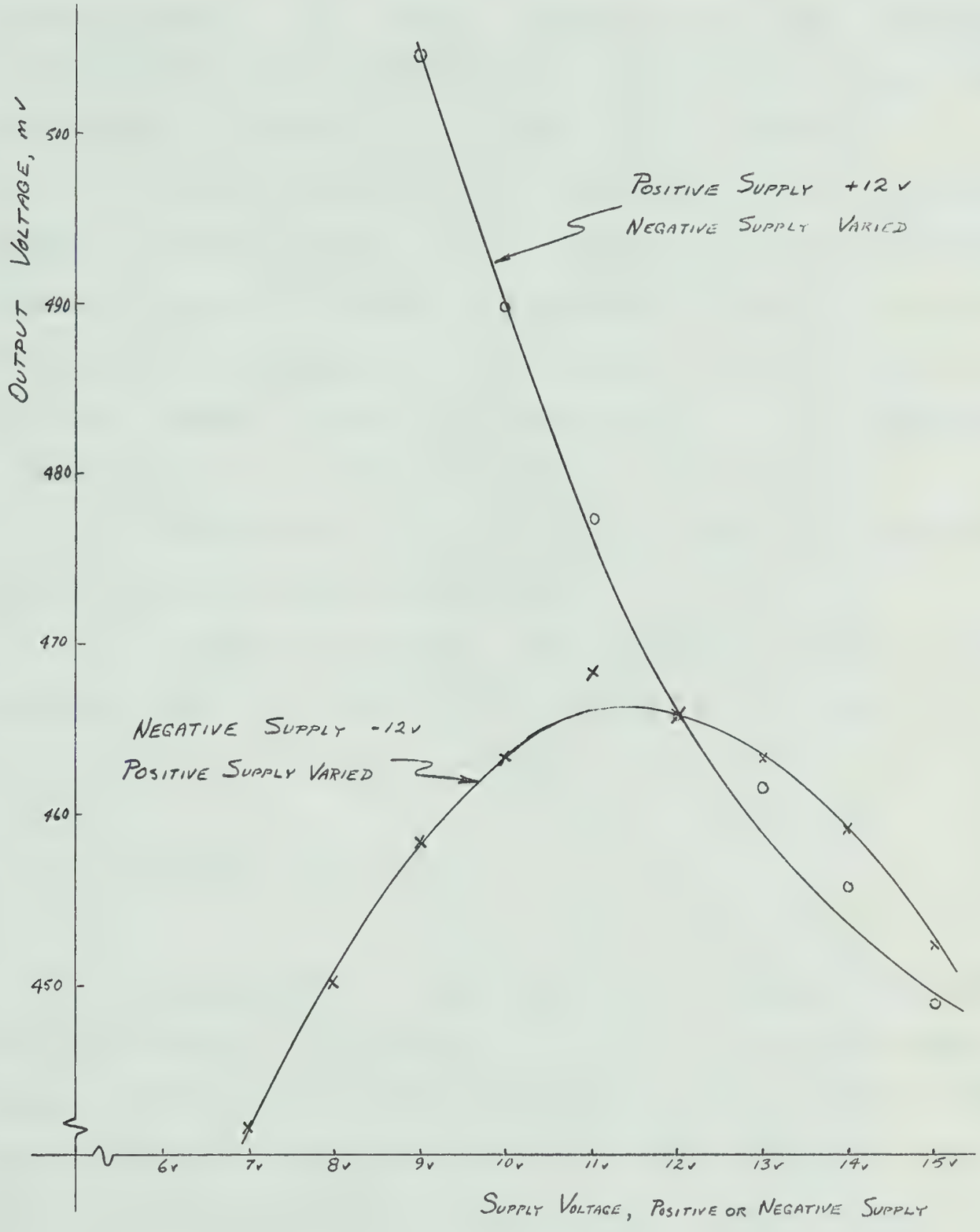

Fig. 6.1 Power Supply Sensitivity of Oscillator Board

the receiver, must be removed until the receiver receives a strong signal. To further conserve power the receiver should operate only a fraction of the time during that period when an interrogation signal is not detected.

The anomalous error in the phase-locked oscillator board should be located. It is possible that a diode phase detector, which is discussed in Appendix II, should be used; with attendant lengthening of the lock signal in order to reliably remove alternating components in the detector output while giving time for transients to die away.

The problem of supply voltage sensitivity could be solved by an unsophisticated regulator.

A photograph of the phase locked oscillator, zero crossing detector and a 100 mw transmitter mounted on a 4 1/2 in. by 6 1/2 in. board is shown in Fig. 6.2.

6.4 Effects of Distortion

In Appendix IV distortion is discussed. From the final expression, an uncertainty of 1.5% in second harmonic content gives rise to 0.2% zero crossing uncertainty or 200 feet. Similarly phase shift of the third harmonic can cause errors. This must be considered in the receiver design.

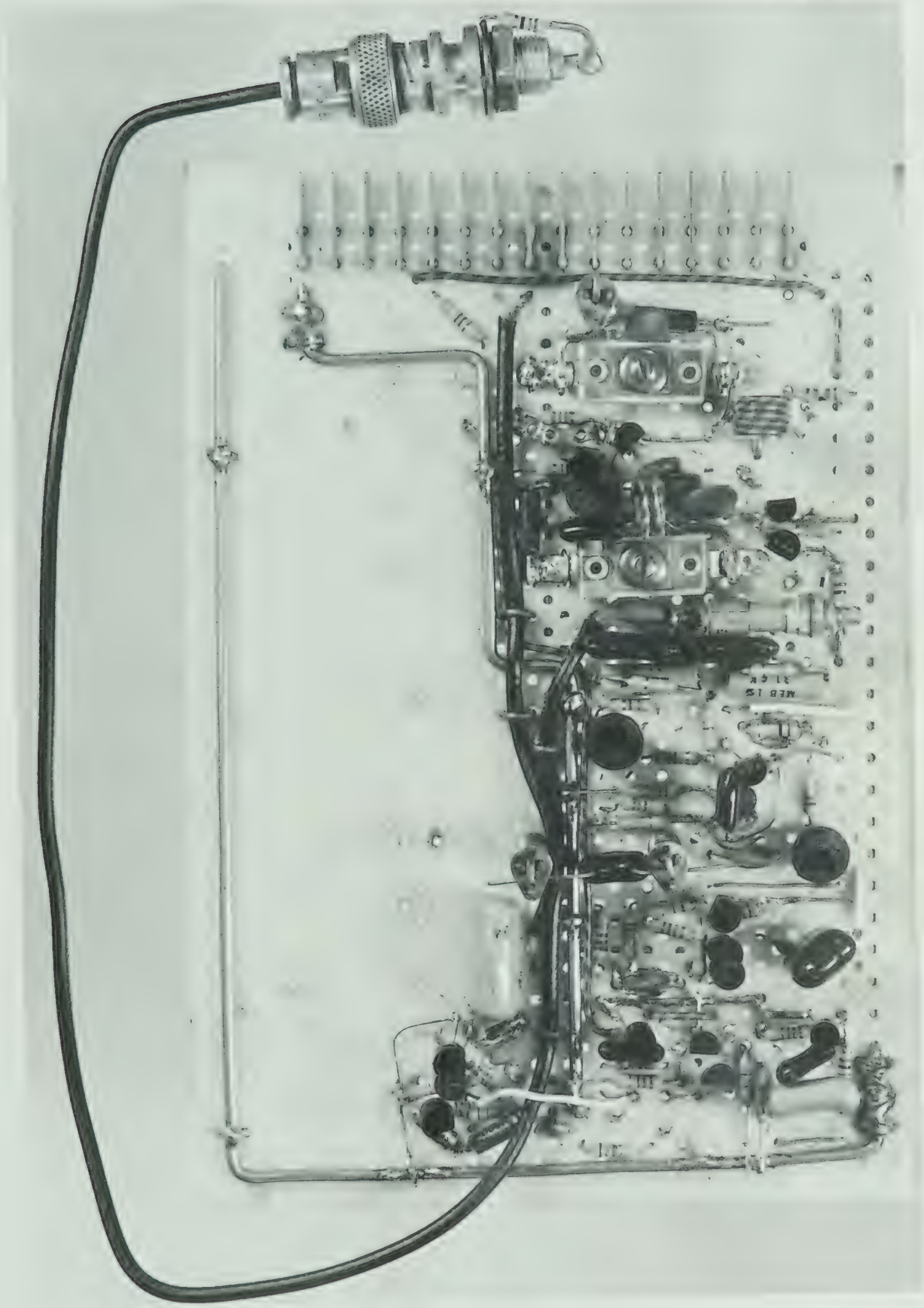

Fig. 6.2 Phase-Locked Oscillator, Transmitter and Zero Crossing Detector

CONCLUSIONS

It has been shown that it is possible to measure distance very accurately using a phase shift transponder with time separation of interrogation and response signals.

The 1/8 mile accuracy at full range will be fairly easily attained, and the accuracy of measurement near the unit will be about 250 feet. RF circuits must be built yet and can further reduce this accuracy, particularly due to uncertainty in the amount that RF interference pulls the frequency during transmission.

The final unit on the collar of the animal will be bulky but lighter than a simple transmitter with this life expectancy and power output.

APPENDIX I

TEST TRANSMITTER

The circuit of Fig. AI.1 was connected to the output of the Wien bridge oscillator of Fig. 5.1. It transmits an amplitude modulated 27.125 MHz from an antenna or into a dummy load. The carrier freqency is determined by X_1 and the modulation is determined by the supply voltage to the class C amplifier. This is the output voltage of the complementary compound emitter follower, whose input is the 10KHz phase-locked sine wave. Since the peak-to-peak voltage output of Q_2 is twice its supply voltage, the modulation is a faithful reproduction of the input signal to the emitter follower.

Q_1 is connected as a common base Colpitts oscillator, with the crystal operating in its series mode. Different crystals gave frequencies within 1KHz of the correct frequency. R_1 supplies enough power to give 24v p/p at the collector. The coil is tapped down to give 5v p/p into Q_2.

Q_2 is a power amplifier driven by Q_1, operating in class C with a short duty cycle. The conduction angle between 40% points is 155^{o} from measurements by

a search coil and sampling oscilloscope. From Scott (Ref. 11) the efficiency using his quartic model for collector current is 68%. The measured efficiency was 65%. Power output was 105mw.

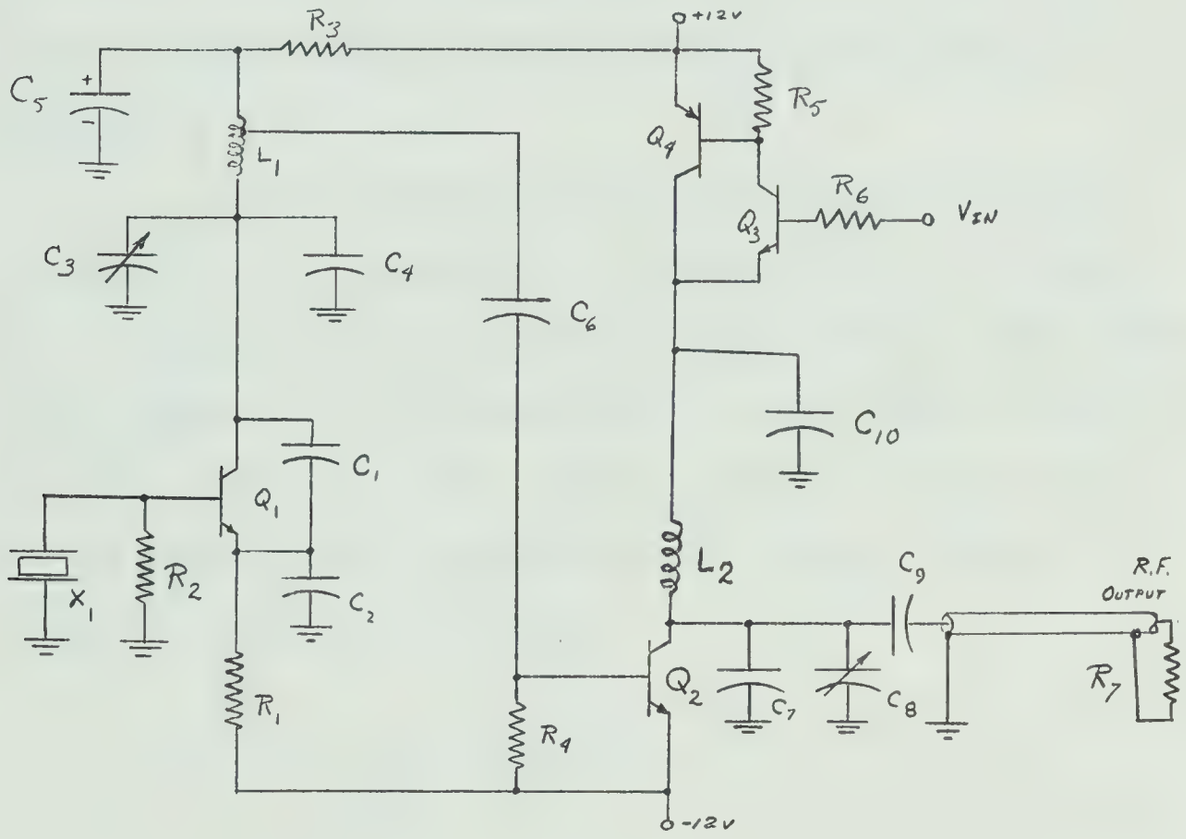

Fig. AI.1 Transmitter Circuit

R_1--1k	R_5--.33k	C_2--100pf	Q_1--2N4401
R_2--2.2k	R_6--10k	C_6--25pf	Q_2--2N4401
R_3--.12k	R_7--51Ω	C_9--33pf	Q3--2N3904
R_4--3.3k	C_1--5pf	C_{10}--1500pf	Q_4--2N3638A

C_3,C_8--Arco 423 trimmer; 8-200 pf

C_4--82 pf silvered mica

C_7--75 pf silvered mica

C_5--1 mfd tantalum electrolytic

X_1--Ch. 14 GRS band, 27.125 MHz

When the envelope was detected, the transmitter was found to have increased the second harmonic distortion by 0.29% and the third harmonic distortion by 0.26%.

At the end of the collector current pulse a spike occurs which generates strong high order harmonics. Using a spectrum analyser the harmonics were -34db with respect to the fundamental for the second harmonic and -28, -32, and -28db for the rest up to the fifth. A well tuned high Q antenna should prevent these harmonics from being radiated.

APPENDIX II

NOISE PERFORMANCE OF PHASE DETECTORS

A2.1 The Sample-Hold Detector

Assume that the input to the zero crossing detector is:

$$V_i(t) = V_s \text{Sin } \omega_i t + n(t)$$

where V_s is the amplitude of the signal and n(t) is the instantaneous noise voltage, and ω_i is the input frequency.

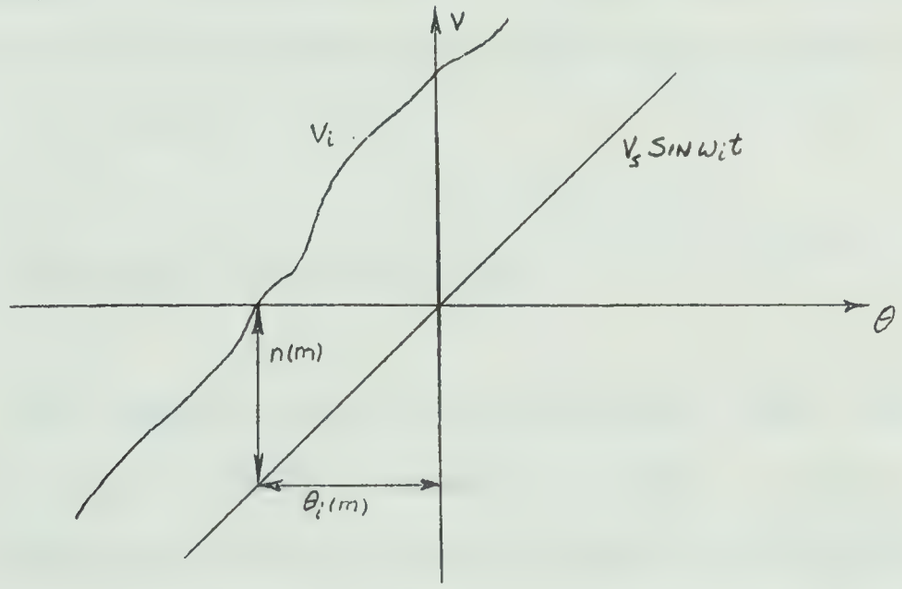

Fig. A2.1 Zero Crossing Error Due to Noise

Let n(m) be the noise voltage at the m'th sampling instant. Then:

$$n(m) = V_s \text{ Sin } \theta_i(m)$$

where θ_i is the resulting zero crossing error.

If $\theta_i(m)$ is small:

$$\theta_i(m) = n(m)/V_s$$

since V_s is a constant the variance of $\theta_i(m)$ is:

$$\overline{\theta_i(m)^2} = \overline{n(m)^2} \; / \; V_s^2 = P_n / \; 2P_s$$

where P_n and P_s are the power in the noise and input signal respectively.

This is identical to the expression that Gardner (Ref. 10) obtained for the linear multiplier. He assumed that the signal has only narrow band gaussian noise associated with it, that the output phase of the VCO is independent of n(t) and that the same linearizing approximation was valid as was made here, ie. $\theta_i \doteq \text{Sin}\ \theta_i$

A2.2 The Diode Phase Detector

The commonly used diode detector (Ref. 10) and the gated amplifier detector as well as some other detectors pass the input signal and noise during an interval p, where p is an appreciable portion of a cycle.

The input voltage distribution function is (Ref. 10):

$$v_i(\omega) = V_s \text{Sin}(\omega_i t - \theta_i)\delta(\omega-\omega_i) + n_c(\omega)\text{Cos}\omega_i t + n_s(\omega)\text{Sin}\omega_i t$$

where $n_c(\omega) = n_s(\omega) = N(\omega)$, which is the noise output of a filter before the phase detector, and $V_s Sin(\omega_i t - \theta_i)$ is the desired input signal.

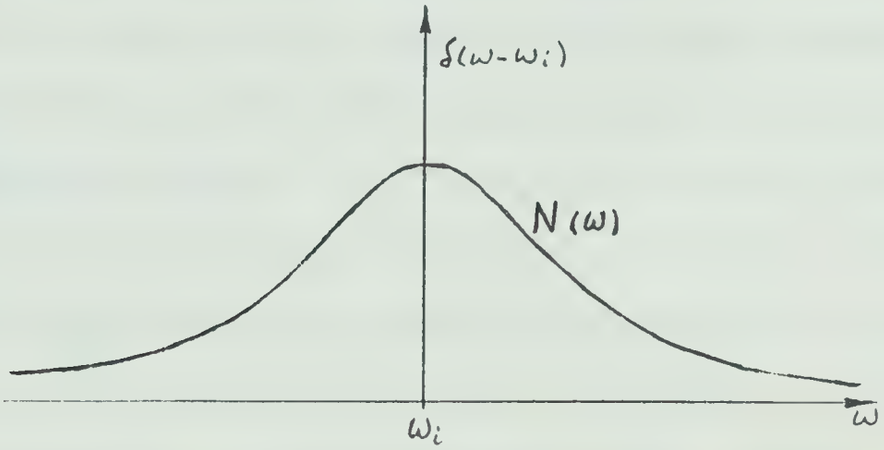

Fig. A2.2 Input Voltage Distribution Function

Since the detector is linear the signal and noise components can be treated seperately. The time integral of the output for one gating interval is given by:

$$v'_{ds} = V_s \int_{-p/2+\theta_o}^{+p/2+\theta_o} Sin(\omega_i t - \theta_i) dt$$

If $_i$ varies slowly it can be treated as constant, and

$$v'_{ds} = \frac{V_s}{\omega_i} \left(Cos(\omega_i p/2 - \theta_i + \theta_o) - Cos(-\omega_i p/2 - \theta_i + \theta_o)\right)$$

Taking the mean and rewriting,

$$v_{ds} = (-p/T_i) V_s \left(\frac{Sin(\pi p/T_i)}{(\pi p/T_i)}\right) Sin(\theta_i - \theta_o)$$

where T_i is the period of v_o, which is assumed to be

locked to v_i. The phase detector gain constant is, if $(\theta_i - \theta_o)$ is small:

$$K_d = (p/T)V_s(\mathrm{Sin}(\pi p/T_i))/(\pi p/T_i)$$

In the limit, where p/T approaches zero, this becomes the same as the sample-hold phase detector with the input rather than the voltage controlled oscillator being sampled. In the usual circuit, the aperture p is approximately T/2 with the zero crossings of the voltage controlled oscillator coinciding with +p/2 and -p/2, and this circuit introduces a 90^o phase shift. The gain is then reduced by the factor $\mathrm{Sin}(\pi/2)/(\pi/2) = 0.637$.

The time integral of the noise voltage distribution due to the m'th pulse is:

$$v'_{d_n}(\omega_n) = n_c\int_{-p/2+\theta_o}^{p/2+\theta_o} \mathrm{Cos}(\omega_n t-\theta_m)dt + n_s\int_{-p/2+\theta_o}^{p/2+\theta_o} \mathrm{Sin}(\omega_n t-\omega_m)dt$$

$$=-n_c p\left(\frac{\mathrm{Sin}(\omega_n p/2)}{(\omega_n p/2)}\right)\mathrm{Cos}(\theta_m-\theta_o) - n_s p\left(\frac{\mathrm{Sin}(\omega_n p/2)}{(\omega_n p/2)}\right)\mathrm{Sin}\,(\theta_m-\theta_o)$$

Where θ_m is the phase shift of the m'th cycle due to the difference between ω_n and ω_i.

$$\Theta_i = 2\Pi m(T_n - T_i)/T_i$$

Since n_s and n_c are uncorrelated and equal, the mean square noise output is:

$$\overline{v_d'^2(\omega_n)} = N(\omega)^2(p/T)^2\left(\frac{\mathrm{Sin}\ (\omega_n p/2)}{(\omega_n p/2)}\right)^2$$

The Θ_m and Θ_o dependence has disappeared and we can integrate with respect to frequency and take the mean to get the mean square detector output.

$$\overline{v_d^2} = \frac{p^2}{T_i^2}\left[V_s^2\left(\frac{\mathrm{Sin}(\omega_i p/2)}{(\omega_i p/2)}\right)^2 \mathrm{Sin}^2(\Theta_i - \Theta_o)\right]$$

$$+ \int_o^\infty N^2(\omega)\left(\frac{\mathrm{Sin}(\omega_n p/2)}{(\omega_n p/2)}\right)^2 d\omega$$

From the last term it is apparent that this phase detector will filter out high frequency noise. If p = T/2 its response is shown in Fig. A2.3.

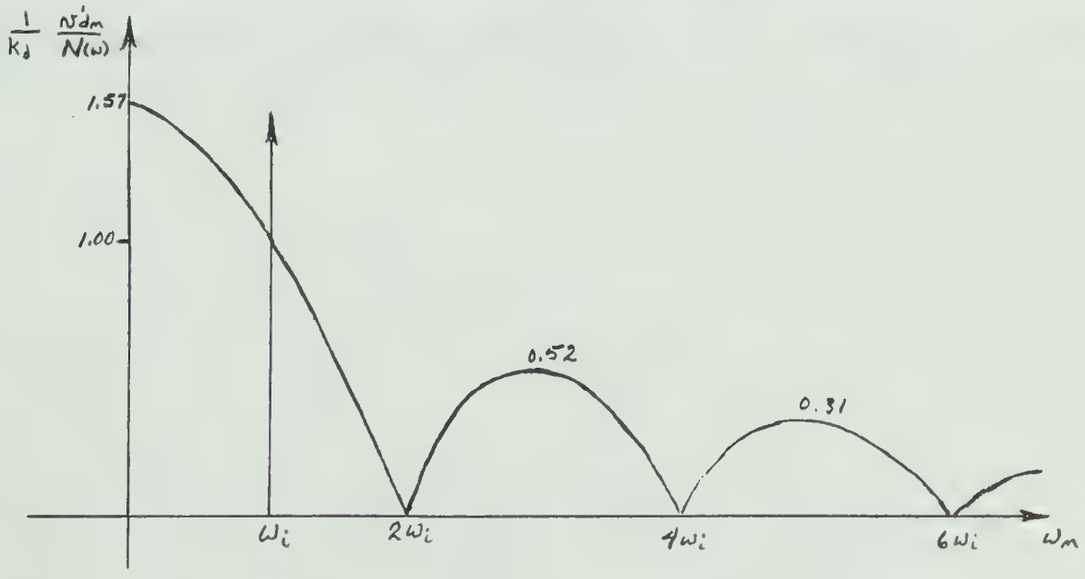

Fig. A2.3 Noise Transfer Function

APPENDIX III

EFFECT OF ENVIRONMENTAL CHANGES

Suppose for some reason such as a temperature change the frequency of the oscillator drifts to ω_o. To return it to resonance requires a control voltage shift, $v_2 = (\omega_i - \omega_o)/k_o = Av_d$. When the loop is closed, a phase error provides v_d,

$$(\theta_i - \theta_o) = v_d/k_d = (\omega_i - \omega_o)/Ak_ok_d$$

Let the frequency control function be expressed in a percentage form:

$$g_o = k_o/\omega_o$$

Then taking logarithmic derivatives:

$$(1/2\pi)d\theta/dE = ((1/\omega)d\omega/dE)(1/2\pi gAV_o)$$

Where dE is an environmental shift.

This shows us that 2π g A V_o gives the percentage reduction in phase shift due to a frequency shift.

APPENDIX IV

EFFECT OF HARMONICS ON ZERO CROSSINGS

Assume that the system receives a signal consisting of a fundamental phase-locked sine wave plus the second and third harmonics.

$$V = V_1 \text{Sin } x - V_2 \text{Cos}(2x+\Phi) + V_3 \text{Sin}(3x+\Theta)$$

$\Phi = 0$ when the second order distortion has been generated by a semiconductor junction, and $\Theta = 0$ when the third harmonic results from an amplifier with an anti-symmetrical characteristic, ie. the Wien bridge. Treating them separately, we can solve for x, the zero crossing error, and add the results, since the linearizing approximation $x = \text{Sin } x$ will be valid and superposition applies.

Considering the second harmonic, the solution x_2 is given by:

$$V = 0 = \text{Sin } x_2 \{V_1 + 2V_2 \text{Sin } x_2 \text{Sin}(x_2+\Phi)\} - V_2 \text{Cos } \Phi$$

Solving:

$$\text{Sin } x_2 \doteq \frac{V_2}{V_1} \text{ Cos } \Phi$$

and $$x_2 \doteq \frac{V_2}{V_1}$$

where $\text{Sin } x_2 \doteq x_2$ because $V_2 << V_1$

and $\text{Cos } \Phi \doteq 1$ because Φ is kept small.

The first approximation is optimistic and distortion

must be less than 10% for 1/2 % accuracy in zero crossing error. The second approximation is conservative. Considering the third harmonic, the solution x_3 is given by:

$$V = 0 = \text{Sin } x_3\{V_1 + 2V_3\text{Cos } x_3\text{Cos}(x_3+\theta)+ V_3\text{Cos}(2x_3+\theta)\} + V_3\text{Cos } x_3\text{Sin } \theta$$

Solving,

$$\text{Sin } x_3 \doteq (V_3/(V_1+3V_3))\text{ Sin } \theta$$

$$x_3 \doteq (V_3/V_1)\ \theta$$

Where $V_3 << V_1$ and therefore $\text{Cos}(x_3+\theta) \doteq \text{Cos } x_3 \doteq \text{Cos}(2x_3+\theta) \doteq 1$ and where θ is assumed to be small and $\text{Sin } \theta \doteq \theta$. Applying superposition, we obtain:

$$x/2\pi \doteq \{(V_2/V_1)+ (V_3/(V_1+3V_3))\text{Sin } \theta\}/2\pi$$

or to less accuracy:

$$x/2\pi = \{(V_2/V_1)+ V_3\theta\}/2\pi V_1$$

Where θ is the phase shift of the third harmonic in radians.

REFERENCES

1. D.B. Siniff and J.R. Tester: 'Computer Analysis of Animal Movement Data Obtained by Telemetry' Bioscience, Feb. 1965.
2. Cochrane et al: 'Automatic Radio-Tracking System for Monitoring Animal Movements', Bioscience, Feb. 1965.
3. Chute, F.S.: 'The Possibility of Using Electromagnetic Momentum to Stabilize a Space Vehicle' PhD Thesis, University of Alberta, 1966.
4. W. W. Cochrane and R. D. Lord: 'Techniques in Radio-Tracking Animals', Reprint from Bio-Telemetry.
5. J.M. Green: Personal Communication.
6. F.E. Terman: Radio Engineer's Handbook, McGraw Hill, 1943 Edition, p 759.
7. Carl H. Nellis, Rochester Wildlife Research Station: Personal Communication.
8. E.M. Edwards: Personal Communication.
9. D.F. Mcfarlane: 'A High Speed Analog to Digital Encoder' MSc Thesis, 1966.
10. F.M. Gardner: Phaselock Techniques, J. Wiley, 1966
11. T.M. Scott: 'Tuned Power Amplifiers' IEEE Transactions on Circuit Theory, Sept. 1964, pp 98-100

B29894